

1 **Introducing standardized field methods for fracture-focused surface**  
2 **processes research**

3 Martha Cary Eppes<sup>1</sup>, Alex Rinehart<sup>2</sup>, Jennifer Aldred<sup>3</sup>, Samantha Berberich<sup>1</sup>, Maxwell P. Dahlquist<sup>4</sup>, Sarah  
4 G. Evans<sup>5</sup>, Russell Keanini<sup>6</sup>, Stephen Laubach<sup>7</sup>, Faye Moser<sup>1</sup>, Mehdi Morovati<sup>6</sup>, Steven Porson<sup>1</sup>, Monica  
5 Rasmussen<sup>1</sup>, Uri Shaanan<sup>8</sup>

6 <sup>1</sup> Department of Geography & Earth Sciences, University of North Carolina at Charlotte, Charlotte, NC 28223, USA

7 <sup>2</sup> Department of Earth and Environmental Sciences, New Mexico Institute of Mining and Technology, Socorro, NM, 87801, USA

8 <sup>3</sup> New Mexico Highlands University, Las Vegas, NM, USA

9 <sup>4</sup> Department of Geology, University of the South, Sewanee, TN 37383, USA

10 <sup>5</sup> Department of Geological and Environmental Sciences, Appalachian State University, Boone, NC, 28608, USA

11 <sup>6</sup> Department of Mechanical Engineering and Engineering Science, University of North Carolina at Charlotte, Charlotte, NC  
12 28223, USA

13 <sup>7</sup> Department of Geological Sciences, University of Texas at Austin, Austin, TX

14 <sup>8</sup> Geological Survey of Israel, Jerusalem 9692100, Israel

15 *Correspondence to:* meppes@charlotte.edu

16

17 **Abstract.** Rock fractures are a key contributor to a broad array of Earth surface processes due to their direct control on rock  
18 strength as well as rock porosity and permeability. However, to date, there has been no standardization for the quantification of  
19 rock fractures in surface processes research. In this work, the case is made for standardization within fracture-focused research,  
20 and prior work is reviewed to identify various key datasets and methodologies. Then, a suite of standardized methods is presented  
21 as a starting ‘baseline’ for fracture-based research in surface processes studies. These methods have been shown in preexisting  
22 work from structural geology, geotechnical engineering, and surface processes disciplines to comprise best practices for the  
23 characterization for fractures in clasts and outcrops. This practical, accessible, and detailed guide can be readily employed across  
24 all fracture-focused weathering and geomorphology applications. The wide adoption of a baseline of data collected using the same  
25 methods will enable comparison and compilation of datasets among studies globally and will ultimately lead to a better  
26 understanding of the links and feedbacks between rock fracture and landscape evolution.

27  
28 **Short Summary.** All rocks have fractures (cracks) that can influence virtually every process acting on Earth's surface where  
29 humans live. Yet, scientists have not standardized their methods for collecting fracture data. Here we draw on past work across  
30 geo-disciplines to show why standardization is important and propose a list of baseline data for fracture-focused surface processes  
31 research. We detail its rationale and the methods for collecting it. We hope its wide adoption will improve future methods and  
32 knowledge of rock fracture overall.

### 33 **1 Introduction**

34 Rock fracture in surface and near-surface environments plays a key role in virtually all Earth surface processes. Fractures comprise  
35 faults and opening-mode fractures; both coming in a wide range of sizes. The focus here is on opening-mode fractures. The  
36 propagation of opening-mode fractures universally occurs at or near the surface of Earth (e.g., within ~500 m - Moon et al., 2020),  
37 on other terrestrial bodies (Molaro et al., 2020), and at depth in the crust (e.g., Laubach et al., 2019). It epitomizes mechanical  
38 weathering and the development of ‘critical zone architecture’, i.e., the evolving porosity, permeability, and strength of near-  
39 surface rock (e.g., Riebe et al., 2021). For clarity and consistency herein, the use of the term fracture is limited to refer to any *open*,  
40 high-length-to-aperture-ratio discontinuity in rock, regardless of its origin, scale, or location (e.g. within a clast, or within shallow  
41 or deep bedrock), acknowledging that veins (partly to completely mineral filled fractures) or dikes (filled with secondary minerals)  
42 are also termed ‘fractures’ in many contexts. The term ‘crack’ is avoided because the wide-ranging semantics of that term can  
43 cause confusion when employed in interdisciplinary work across rock mechanics, structural geology, and geomorphology.

44  
45 Fracture characteristics (e.g. size, number, connectivity, orientation) exert enormous influence on both rock mechanical properties  
46 (e.g., Ayatollahi and Akbaridoost, 2014) and rock hydrological properties (e.g., Leone et al., 2020; Snowdon et al., 2021). Fractures  
47 therefore influence a wide array of natural and anthropogenic landscape features and processes including channel incision (e.g.,  
48 Shobe et al., 2017), sediment size and production (Sousa, 2010; Sklar et al., 2017), hillslope erosion (e.g., DiBiase et al., 2018;  
49 Neely et al., 2019), built environment degradation (e.g., Hatir, 2020), landslide and rockfall hazards (e.g., Collins and Stock, 2016),  
50 groundwater and surface water processes (e.g., Maffucci et al., 2015; Wohl, 2008), and vegetation distribution (e.g., Aich and  
51 Gross, 2008). Additionally, the resultant physical properties of fracturing-produced sediment (i.e., clast size distribution, mass,  
52 porosity, etc.) control both hillslope and stream processes (e.g., Chilton and Spotila, 2020; Glade et al., 2019).

53

54 With fractures clearly central to so many surface processes, as well as to non-academic concerns of hazard and infrastructure  
55 degradation, it is crucial to understand the factors that control surface and near-surface rock fracture attributes and rock fracturing  
56 rates and processes. To fully do so requires a large body of data quantifying fracture-related characteristics and phenomena in a  
57 variety of subaerial environments; however, to date, no standard field methods have been widely adopted to quantify fractures in  
58 the modern surface processes realm. Consequently, data collected across studies cannot be readily compared or coalesced. The  
59 purpose of this paper is to define an initial set of such standards with the anticipation that they can and should change over time as  
60 understanding evolves. We develop these proposed standards by combining prior fracture methodologies from other geoscience  
61 disciplines with those that have been developed, tested and refined through more than 20 years of field-based fracture observations  
62 for surface processes-related research (e.g., Aldred et al., 2015; Eppes and Griffing, 2010; Eppes et al., 2018; Eppes et al., 2010;  
63 Mcfadden et al., 2005; Moser, 2017; Shobe et al., 2017; Weiserbs, 2017).

64  
65 Building on this combination of past work, this paper defines the benefits of establishing a standard procedure for fracture-focused  
66 surface processes field research, describing how the authors' chosen methods outperform other approaches. We then present a  
67 short review of motivating existing approaches derived primarily from engineering and structural geology disciplines. Finally, we  
68 define a set of methods that is proposed as a starting point for surface processes researchers so that a larger community of teams  
69 can begin to cross-pollinate their observations. It is necessary and expected that the methods will evolve as new needs and  
70 applications arise. The overall scope herein is limited to in-person field observations on sub-aerially exposed rock, i.e., fractures  
71 that can be observed with the naked eye or basic hand lens. Measurements of smaller fractures (e.g., those visible with microscopy)  
72 or of buried fractures (e.g., those visualized in boreholes or with indirect geophysical methods) are not directly described here.

73  
74 We also note that methods for fracture detection using automated analyses of remote data such as LiDAR, drone photography,  
75 structure-from-motion, or 3D modeling are not described herein. These technologies, which enable the production of fracture maps  
76 whose properties can then be quantified and characterized digitally using freely available software packages such as FracPaQ  
77 (Healy et al., 2017), are rapidly evolving and hold great promise for expanding the scope of fracture measurements overall (Betlem  
78 et al., 2022; Zeng et al., 2023). To date, however, mapping fractures using these techniques holds limitations such as difficulty  
79 distinguishing between fractures and edges. Thus, the methods outlined herein represent a consistent set of methods that could be  
80 employed for validation across all such remotely sensed data collection. Furthermore, many of the field methods described herein,  
81 such as site and observation area selection, are required for any fracture mapping effort regardless of technique. Thus, many of the  
82 methods we present can be applied to most studies using these rapidly evolving remote sensing technologies, and should aid in  
83 accelerating their development.

84  
85 The overall aim of this paper is to build: 1) a set of guiding principles applicable to all surface processes research involving rock  
86 fractures; 2) a list of fracture and rock data measurements that constitute "basic" field-based metrics; and 3) practical methods that  
87 comprise best practices for collection of these data. Unless otherwise specified, all methods may be applied to loose clasts or to  
88 outcrops. Also provided are some suggestions for data analyses and a demonstration of a real case example of how the proposed  
89 methods lead to reproducible results across users. By providing this compendium of fracture-focused field methods, the hope is to  
90 accelerate understanding of how a most basic feature of all rock – its open fractures – contributes to the processes and evolution  
91 of Earth's surface and critical zone.

## 92 1.1 The value of a standardized approach

93 Particularly within the fields of geomorphology and weathering sciences, no common suite of data, methods, or terminology has  
94 been defined or described that comprises an analysis of fractures. Although fracture characterization field methods exist in the  
95 context of structural geology and aquifer and reservoir characterization (e.g., Watkins et al., 2015; Wu and Pollard, 1995; Zeeb et  
96 al., 2013; Laubach et al., 2018), they diverge significantly in their approaches because they were largely developed for the specific  
97 application of each unique study or field of study. Furthermore, the terminology and methodology used to describe natural fractures  
98 across this existing research tend to focus on what are typically envisioned as deep-seated processes including tectonic loading and  
99 pore pressure elevation (e.g., Schultz, 2019). Numerous published works fail to provide clear criteria for categorizing fractures,  
100 or even for choosing which fractures to measure. The choices, of course, depend on the objectives of the study. This lack of  
101 consistency severely limits the ability of the geomorphic community to reproduce methods, or to combine, compare, or interpret  
102 different fracture datasets.

103  
104 The development of consistent methods undergirds most quantitative Earth sciences. For example, the fields of sedimentology and  
105 soil science have clear, standardized methods to acquire what constitutes the “basic” data for their observations. Sedimentologists  
106 have long shared common metrics and methods for quantifying grain size, sorting, rounding, and stratigraphic records (e.g.,  
107 Krumbein, 1943). Similarly, soil scientists share common methods, metrics, and nomenclature for describing soil profiles and  
108 horizons (e.g., Birkeland, 1999 Appendix A; Soil Survey Staff, 1999). The realization of the need for standard methods has also  
109 remained constant in laboratory-based rock mechanics over the last several decades, driving the American Society for Testing and  
110 Materials (ASTM) and International Society for Rock Mechanics (ISMR) to publish ongoing standards and methods papers (e.g.,  
111 Ulusay and Hudson, 2007; Ulusay, 2015).

112  
113 Standards like those mentioned above exist because workers have long recognized and reaped their benefits. Standardized methods  
114 can frequently lead to major step-change innovations when data are combined. For example, standardized soil methods allowed  
115 for 100 m scale mapping across the United States, enabling detailed human–landscape models that can aid in preserving vital soil  
116 resources (Ramcharan et al., 2018). In the field of rock mechanics prior to the 1950s, theoretical developments of rock failure and  
117 plasticity lagged other branches of geophysics and engineering, limited both by technology but, arguably more so, by lack of  
118 consistent methods. Methods for repeatable failure testing were then developed, largely in the groups led by Knoppf, Griggs, and  
119 Turner in the United States and Australia (Wenk, 1979). This standardization culminated in the landmark series of papers that  
120 comprised the observations driving 50 subsequent years of experimental rock mechanics (e.g., Borg and Handin, 1966; Handin et  
121 al., 1963; Handin and Hager, 1957, 1958; Heard, 1963; Mogi, 1967, 1971; Turner et al., 1954).

## 122 123 124 1.2 Development of the standardized fracture measurement approach

125 For the specific case of fracture-focused research, outside of geomorphology applications, the need for standardized rule-based  
126 methods has already been established. Within this prior body of research, engineering and structural geology applications have  
127 dominated the development of various approaches.

128

129 Engineering geology and geotechnical engineering share common practices in mapping different standards of rock quality and  
130 rock mass classification, of which fracture characterization is an important component. The rock quality designation (RDQ) was  
131 developed in the early 1960s to predict rock mass suitability for building, foundations, tunneling, and other geotechnical issues  
132 (Deere, 1964 in Bell, 2007). Within that work, the primary concern is the integrity of the rock, which is governed by its  
133 discontinuities, primarily fractures. By providing a standard approach to defining rock quality - albeit qualitative or semi-  
134 quantitative - the development of a globally accepted basis of rock mass classification built from RQD and discontinuity surveys  
135 has provided a common language for engineering geologists and geotechnical engineers to discuss site suitability and to design  
136 critical infrastructure to the point that slope stability parameters, hydrologic suitability and intact strength can be broadly predicted  
137 (Bell, 2007; Hencher, 2012; Hencher, 2015). Thus, these rock quality metrics may be appropriate for surface processes applications,  
138 and they provide a rationale and a basis for the use of the semi-quantitative methods presented herein.

139  
140 The rock quality index consists of qualitative classifications from very poor (RQD 0 to 25%) to excellent (RQD 90 to 100%) based  
141 on the linear fracture frequency in core or outcrop line surveys, laboratory velocity measurements, or the ratio of the deformability  
142 of the rock mass to that of intact rock (Bell, 2007). Specifically for fractures, rock quality designations are derived only from counts  
143 of the number of fractures per foot or core or outcrop. More quantitative estimates of outcrop rock mass quality – commonly used  
144 to estimate slope stability quantities – involve measuring multiple lines on an outcrop with estimates of fracture aperture width,  
145 hydrologic state (closed, cemented, partially open, open and flowing), fracture orientation, strength of intact rock estimated with a  
146 rock hammer, degree of weathering, and fracture ‘roughness’ or relief along a line of a fixed length, commonly 20 m to 30 m (Bell,  
147 2007). These surveys are then repeated periodically with a spacing of ~100 m, depending on the application (Bell, 2007). Similar  
148 methods are used with core and image logging tools (Hencher, 2012; Hencher 2015). The fracture parameters are then used in a  
149 variety of index models that predict the bulk strength, hydraulic conductivity, and stability of the rock mass. Thus, the extensiveness  
150 of the list of measured rock- and fracture- characteristics reflects the variety of impacts that they have both on each other and on  
151 the behavior of the rock mass. Here a similar comprehensive list is proposed, but more with surface processes applications in mind.

152  
153 Measurements of the length and aperture of fractures that intersect a line (scanlines), similar to those used for engineering rock  
154 quality applications, are widely used and effective in structural geology applications (Marrett et al., 2018; Hooker et al., 2009),  
155 and may be valuable where exposures approximate a 1D sample. Selection bias can be avoided by randomly picking scanline  
156 directions or by measuring multiple scanlines. To capture all fracture orientations geometric corrections are needed (e.g., Terzaghi,  
157 1965; Wang et al., 2023). When fractures are oblique to scanlines, these corrections are generally more effective if scanlines are  
158 long relative to fracture occurrence. Calculations of fracture number density and fracture intensity (Sect. 6.1) require corrections  
159 for comparison with 2D data. Depending on the heterogeneity and anisotropy of host rocks, long 1D measures may complicate  
160 comparison of fracture patterns to rock properties. Although they are well suited for capturing the most reproducible and unbiased  
161 measure for fracture size, namely fracture aperture distributions (e.g., Marrett et al., 2018) as a 1D measure, without extra  
162 measurement steps, scanlines are not well suited for characterizing representative 2D or 3D rock characteristics or for measuring  
163 fracture lengths, heights, or connectivity, all important to surface processes. Thus, in the proposed methods herein, the focus is on  
164 2D ‘windows’, and an expansion of fracture length measurements – like that proposed by Weiss (2008) – is also detailed so that  
165 long fractures are not underrepresented (see Sect. 5.4.1 for length methods).

166

167 For 2D characterizations, Zeeb et al. (2013) sought to determine how different sampling approaches lead to censoring bias of  
168 different fracture sizes from outcrop data by applying different sampling methods to artificially generated fracture networks that  
169 had known parameters. Analysis of data collected using scanline, window, and circular estimator methods revealed that the window  
170 approach resulted in the lowest uncertainty for most parameters and required the fewest measurements to provide representative  
171 datasets. For areas with large outcrop exposures, circular scanlines combined with a window approach have proven effective  
172 (Watkins et al., 2015). Scanlines are also helpful in characterizing simple fracture spatial arrangement attributes. Here, a ‘window’  
173 approach is outlined that can be employed regardless of outcrop size or fracture number density.

174  
175 Another consideration that arises in both structural geology and the engineering applications is that the methods of fracture (and  
176 rock) characterization must include accommodation for rock variations, and discipline-specific considerations for specific sites  
177 (Hencher, 2012). In particular, the total area(s) of observation and numbers of fractures examined must always be normalized for  
178 the specific rock and/or location within the ‘fracture stratigraphy’ of a study (e.g., Laubach et al., 2009). For example, it is common  
179 for sandstone and shaly sandstone to both occur over short distances and that their fracture abundance will vary by rock type (for  
180 example, clay-poor sandstones tend to be more brittle and fracture prone). In this circumstance, the lithologic control on abundance  
181 is identified first (this can be qualitative), then the abundance measures are normalized to area of the specific rock type. For  
182 example, Hooker et al. (2013) employs a reverse procedure, whereby multivariate measures are used to isolate the rock type to  
183 which normalization should be confined (if any). A further caution is that all fracture populations in the same rock may not reflect  
184 the attributes of the host rock in the same way (all parts of the fracture population may not even be present in all rock types). This  
185 variance may arise if fractures are not all of the same age; because differences in loading paths, exposure histories, and rock  
186 properties may vary. Engineering geology applications often map fracture populations in a similar way (Hencher, 2012; and  
187 Hencher 2015) but without the geologic context; zones are identified and cross-cutting relationships of fractures are commonly  
188 used to identify primary vs. secondary planes of weakness. The methods presented herein include instructions for how to make  
189 these overall judgements of necessary accommodations and normalizations.

190  
191 Just as fracture characterization methods must be developed to accommodate variance between and across rock types, they must  
192 also be developed so that they are reproducible across users. Above all, it has been established that reproducibility requires clear,  
193 rule-based criteria for all decision-making (Forstner and Laubach, 2022). Forstner and Laubach (2022) and Ortega and Marrett  
194 (2000) detail issues that arise, particularly from a lack of specificity with respect to identifying features to be measured. In another  
195 case example (Andrews et al., 2019), study participants were asked to measure fractures with no particular instructions given for  
196 how to collect the data other than where to collect it. The wide variance in resulting datasets collected by different users led to the  
197 conclusion that, without common and clearly established measurement and selection criteria, fracture characterization is rife with  
198 subjective bias that severely impacts interpretations of results. Then, based on post-data collection interviews and workshops,  
199 Andrews et al. (2019) scrutinized the source of the variance and provided a list of suggested best-practices that would serve to best  
200 eliminate the subjectivity of data collection that was leading to the bias. In engineering contexts, it is more common for fracture  
201 mapping during site investigations to be performed by a single engineering geologist or by a single, small team of trained engineers  
202 or geologists (Hencher, 2012), which ideally would be carefully reviewed by a senior engineering geology professional. These  
203 fracture maps are incorporated into the site model, which is updated – preferably by the same engineering geologist – during  
204 construction. In case studies, it is common for poor quality or inconsistent fracture mapping to lead to incorrectly designed

205 structures, which may fail (Hencher, 2012). Despite these often-dramatic failures, the site-specific nature of fracture networks  
 206 during rock mass characterization and the balance for a financially successful project may lead to poor review and oversight  
 207 practices while developing a site model (Hencher, 2012). Here, so that users from different groups may consistently employ this  
 208 field guide, clear, rules-based criteria are provided that may be used for all measurements described and justify the criteria based  
 209 on past work and experience.

210  
 211 Including that described above, incorporated in this work are suggested best practices from existing published methods research.  
 212 For example, field measurement ‘crack comparators’ are effective for measuring opening displacements particularly for sub-  
 213 millimeter widths (e.g., Ortega et al., 2006). Other measurements such as length and connectivity may have low reproducibility  
 214 (Andrews et al., 2019) owing to various observational and conceptual problems, including dependence on scale of observation  
 215 (e.g., Ortega and Marrett, 2000).

216  
 217 In all cases, the chosen standardized methods presented are optimized for collecting outcrop- and clast-fracture data relevant to  
 218 geomorphology and other surface process-based disciplines (e.g. critical zone sciences, building stone preservation, hydrogeology).  
 219 The methods described herein are germane to surface and near-surface (< 0.5 km) studies such as validating geophysical  
 220 measurements, testing factors that influence fracture formation, or documenting links between fracture characteristics and  
 221 topography or sediment production. These methods possibly differ from those of studies with other goals, such as using outcrops  
 222 as guides (analogs) for deep (km scale) subsurface fractures. Such studies aim to distinguish mechanical and fracture stratigraphy,  
 223 corroborate fracture patterns related to features (i.e., folds or faults), obtain fracture statistics for discrete fracture models, or test  
 224 efficacy of forward geomechanical fracture models. For these studies examining deeper deformation, mineral filled fractures may  
 225 be more useful or appropriate than focusing solely on open fractures. Also, for deep-Earth applications, near-surface and  
 226 geomorphology-related fractures are considered “noise” and need to be omitted (e.g., Sanderson, 2016; Ukar et al., 2019). Yet,  
 227 fractures that are noise to those interested in the deep subsurface are essential features in the context of geomorphology and critical  
 228 zone sciences. A major outstanding question is how this differentiation might be reasonably and accurately accomplished given  
 229 the relatively sparse number of studies of fractures in the context of geomorphology. We hope future workers using this guide may  
 230 find the answers.

## 231 **2 Standardized methods: Guiding principles**

### 232 **2.1 Natural rock fracturing background**

233 The design of any fracture-related study in the context of surface processes must arise from consideration of the variables that may  
 234 influence the rates of fracturing and the characteristics of the fractures that form. When rock is proximal to Earth’s surface, those  
 235 variables include factors related to Earth’s topography, atmosphere, biosphere, cryosphere, and/or hydrosphere. Here, a very brief  
 236 overview is provided of some key rock fracture mechanics concepts behind these factors. Eppes and Keanini (2017) and Eppes  
 237 (2022) provide more detailed reviews of rock fracture processes in the context of surface processes.

238  
 239 Rocks fracture at and near Earth’s surface in response to the complex sum of all tectonic (e.g., Martel, 2006), topographic (e.g.,  
 240 St. Clair et al., 2015; Moon et al., 2020; Molnar, 2004), biological (e.g., Brantley et al., 2017; Hasenmueller et al., 2017), and  
 241 environment-related (e.g., Matsuoka and Murton, 2008; Gischig et al., 2011) stresses they experience. Fracturing can occur when

242 stresses exceed the failure criteria (i.e., short-term material strength). More commonly, however, because critical stresses are rarely  
243 reached in nature, fractures can also propagate *subcritically* at stresses as low or lower than 10% of the rock's strength (see  
244 textbooks such as Schultz, 2019; Atkinson, 1987).

245  
246 Overall, subcritical fracture propagation rates and processes are strongly dependent on stress magnitude, but they are *also* strongly  
247 influenced by the size of the fracture that is under stress (see fracture mechanics textbooks such as Anderson, 2005; or reviews  
248 such as Laubach et al., 2019). For single isolated fractures, stresses applied to the rock body are concentrated at fracture tips  
249 proportional to the length of the fracture (a concept embodied by the term 'stress intensity'), effectively increasing the stresses  
250 experienced by that fracture. Simultaneously, as the entire group of fractures within the rock body grows, the rock can become  
251 'tougher' – more resistant to further brittle failure under the same magnitudes of stresses, as the total rock mass becomes more  
252 compliant (Brantut et al., 2012). Overall, the time-dependency of these interacting and contrasting behaviors is not well  
253 characterized in natural settings.

254  
255 In addition to fracture geometry, environmental conditions also strongly impact fracture tip bond breaking during subcritical  
256 fracture. The environmental factors known to impact subcritical rock cracking - separate from their influence on stresses - include  
257 vapor pressure, temperature, and pore-water chemistry (Eppes and Keanini, 2017; Eppes et al., 2020; Brantut et al., 2013; Laubach  
258 et al., 2019). Therefore, in the context of surface processes, climate matters twice for rock fracturing: 1) as it contributes to the  
259 stresses that the rock experiences, and 2) as it contributes to the chemo-physical processes that break bonds at fracture tips as they  
260 propagate subcritically.

261  
262 Just as other common physical properties like tensile strength can be measured, rocks can be tested for their propensity to fracture  
263 subcritically by the measurement of subcritical cracking parameters such as the subcritical cracking index (e.g., Paris and Erdogan,  
264 1963; Chen et al., 2017; Holder et al., 2001; Nara et al., 2012; Nara et al., 2017). These parameters influence both the rate of  
265 subcritical cracking in rock and the fracture characteristics (e.g., amount of fracture per area or fracture length as in Olson, 2004).

266  
267 In sum, natural rock fracturing is not necessarily the singular, catastrophic event as it frequently portrayed in surface processes  
268 research. Instead, it is likely dominantly a slowly evolving process progressing over geologic time as has been recognized from  
269 fracture patterns in bedrock (e.g. Engelder, 2004; Rysak et al., 2022), and more recently in the context of surface processes  
270 (Shaanan et al., 2023). Importantly, however, there is currently little field-based data elucidating these complex, experimentally  
271 observed phenomena in surface processes contexts. It is our hope that this guide will enable more workers to document the complex  
272 feedbacks between rock and fracture properties, as well as environmental, topographic, and tectonic factors, that likely influences  
273 all fracturing at and near Earth's surface.

## 274 **2.2 Site selection and study design using a “State Factor” approach**

275 Due to their influence on rock fracturing as described above, all potential driving stresses and variations in fracture environments  
276 must be considered in site selection and study design for any fracture-related research. Parent rock, topography (and other loads),  
277 climate, biota, and time all potentially impact initiation and propagation of surficial fractures in rocks. Though this idea might  
278 generally exist in other fracture-focused research, in the field of soil geomorphology it has long been explicitly described as a



279 ‘State Factor’ approach (e.g., Jenny, 1941; Phillips, 1989) to understanding progressive chemical and physical alteration processes.  
 280 Thus, we propose that this well-vetted conceptual paradigm may be employed in fracture-focused surface processes research as a  
 281 standard.

282  
 283 Here, it is asserted that applying a State Factor approach to fracture research is relevant because fracturing processes are influenced  
 284 by each of these factors, just as all other chemical processes acting on rock and soil. This is particularly true when the subcritical  
 285 nature of rock fracture is considered (Sect. 2.1). Thus, all State Factors that could contribute to fracture propagation styles, and  
 286 rates should be explicitly considered and controlled for as much as possible within the aims and scope of the research for any given  
 287 site. These ‘State Factors’ - long categorized as they relate to overall soil development, of which physical weathering is a  
 288 component (e.g., Jenny, 1941) - are equally applicable to fractures alone, and include climate (cl, both regional climate and  
 289 microclimate), organisms (o, flora and fauna), relief (r, topography at all scales), parent material (p, rock properties) and time (t,  
 290 exposure age or exhumation rate). For rock fracture, tectonics (T) should be added to this list, making cl,o,r,p,t,T.

291  
 292 Hereafter, the term ‘site’ refers to a single location of either a group of rock clasts or a group of outcrops, whereby all clasts or  
 293 outcrops within the ‘site’ could be reasonably assumed to have experienced similar State Factors over their exposure history. For  
 294 example, a site might comprise a single boulder bar on an alluvial fan surface or a single ridgeline with several outcrops. Once the  
 295 specific State Factors (including the internal variability of each site) are identified for all the sites within a given field area, a series  
 296 of sites can be selected whose State Factors are known and controlled for as much as possible. This enables a study of the influence  
 297 of individual factors across the sites, i.e., fracture chronosequences, climosequences, toposequences, or lithosequences.

298  
 299 For rock fracture, it is important to understand how each cl,o,r,p,t,T factor may contribute both to stresses that give rise to fracturing,  
 300 and/or to the molecular-scale processes that serve to subcritically break bonds at fracture tips (Sect. 2.1). Each has the potential to  
 301 independently impact fracturing rates, styles, and processes. The following descriptions provide only brief examples of how each  
 302 of the State Factors may influence rock fracture. To fully describe each of their influences on rock fracturing would comprise a  
 303 textbook. The factors are listed in the cl,or,r,p,t,T order by traditional convention only. Assuredly, to date, there are insufficient  
 304 data to propose a hierarchy of their influence on fracture characteristics in surface processes contexts.

### 305 2.2.1 Climate (cl)

306 *Climate (cl)* as a State Factor refers not just to regional mean annual precipitation or temperature, but also the local microclimate  
 307 of a site, which may be influenced by site characteristics, such as runoff or aspect. The presence of liquid water increases the  
 308 efficacy of water-related stress-loading processes like those related to freezing (Girard et al., 2013) or chemical precipitation of  
 309 salts or oxides (e.g., Buss et al., 2008; Ponti et al., 2021). Moisture – particularly vapor pressure – can also serve to accelerate rock  
 310 fracturing rates independent of any stress-loading (e.g., Eppes et al., 2020; Nara et al., 2017). Temperature cycling can produce  
 311 thermal stresses (through differential expansion and contraction of both adjacent minerals as well as different portions of the rock  
 312 mass, e.g., Ravaji et al., 2019), and can also influence rates and processes of fracture-tip bond breaking (e.g., Dove, 1995).

### 313 2.2.2 Organisms (o)

314 *Organisms (o)* refers to both flora and fauna - everything from overlying vegetation and large animals to roots and microorganisms,  
 315 all of which may provide a source of rock stress and/or may influence water availability or chemistry. These relationships can be  
 316 complex and unexpected. For example, tree motion during wind and root swelling during water uptake both exert stresses on rock  
 317 directly (Marshall et al., 2021a). Organism density and type can impact rock water and air chemistry (Burghelca et al., 2015), both  
 318 of which may impact the rates and processes of subcritical cracking (e.g., review in Brantut et al., 2013).

### 319 2.2.3 Relief (r)

320 In the context of State Factors, *relief (r)* refers generically to all metrics related to topography including aspect, slope, and  
 321 convexity. Topography impacts the manifestation of both gravitational stresses, as well as tectonic stresses within the rock body  
 322 (Molnar, 2004; Moon et al., 2020; Martel, 2006). The directional aspect of a particular outcrop or boulder face may also influence  
 323 insolation and water retention, translating into differences in microclimate and vegetation and, thus, weathering overall (e.g.,  
 324 Burnett et al., 2008; West et al., 2014; Mcauliffe et al., 2022), including fracturing (e.g., West et al., 2014).

### 325 2.2.4 Parent material (p)

326 The *parent material (p)* factor in the context of a fracture study refers to the specific rock type(s) containing fractures (and  
 327 potentially undergoing fracture) in the geomorphic environment. Rock varies in the types and dimensions of material present (e.g.,  
 328 sandstone, siltstone, shale, basalt, granite etc.) and the types and spatial arrangements of interfaces within the material (e.g., grain  
 329 size, porosity, bedding, foliation). These properties directly influence the rates and styles of fracture propagation (Atkinson, 1987)  
 330 due to both how they respond to stresses but also due to how they allow stresses to arise. Thus, they can all influence the rates and  
 331 characteristics of fracture growth and susceptibility to topographic and environmental stresses. For example, different minerals are  
 332 characterized by different coefficients of thermal expansion. As a result, rocks with different mineral constituents will be more or  
 333 less sensitive to thermal stresses than others depending on the contrasts between adjacent grains. Rock mineralogy will also impact  
 334 chemical processes acting at crack tips during subcritical cracking, as well as the overall susceptibility of the rock to chemical  
 335 weathering.

336  
 337 Many (perhaps most) rocks contain fractures that formed prior to exposure, either due to deep seated tectonics and fluid pressure  
 338 loads or to thermal and mechanical effect due to uplift towards the surface (English and Laubach, 2017; Engelder, 1993). In  
 339 sedimentary rocks, fracture patterns (and, in some cases, fracture stratigraphy) vary with mechanical stratigraphy (e.g., Laubach et  
 340 al., 2009) that can also influence near-surface fracture. In many instances, mechanical properties may be reflected in fracture  
 341 stratigraphy, and vice versa. Schmidt hammer measurements are a useful, fast, and inexpensive field approach to documenting  
 342 mechanical property variability (Aydin and Basu, 2005), however such measurements are impacted by weathering exposure age  
 343 (e.g. Matthews and Winkler, 2022). The influence of fracture characteristics of the parent rock that may have formed in the deep  
 344 subsurface are described in Sect. 2.2.6 “Tectonics”.

345  
 346 Additionally, here, parent material also refers to the size and shape of the clast or outcrop. For example, angular corners generally  
 347 concentrate stresses more than rounded edges (Anderson, 2005). Also, clasts or outcrops of different sizes experience different  
 348 magnitudes of thermal stresses related to diurnal heating and cooling (Molaro et al., 2017).

### 349 2.2.5 Time (t)

350 *Time (t)* likely plays a role in rock fracturing rates just as it does in chemical weathering, whereby outcrops found in slowly-eroding  
 351 environments or clasts on old surfaces may be subject to different fracturing rates and processes (e.g., Rasmussen et al., in review;  
 352 Mushkin et al., 2014). Over time, rock mechanical properties can also change as weathering occurs (e.g., Cuccuru et al., 2012).  
 353 Although the time factor has not been well-studied in the context of natural rock fracture, preliminary data suggest that it should  
 354 be considered (Berberich, 2020; Rasmussen et al., 2021). Published surficial geologic maps or datasets of rock exposure ages or  
 355 erosion rates (e.g., Balco, 2020) can provide ‘time’ information.

### 356 2.2.6 Tectonics (T)

357 Finally, in a fracture-related study, *tectonic (T)* setting must also be considered as a State Factor. Fractures that have formed in the  
 358 deep to near subsurface in response to tectonic forces such as plate-scale stress fields, folding, and faulting (and attendant pore  
 359 pressure variations) may continue to propagate at or near the surface; and they inevitably become exhumed. Overall, fractures  
 360 formed by these processes have traditionally been studied within the structural geology discipline, and that literature is extensive  
 361 (e.g., reviews in Laubach et al., 2019; Laubach et al., 2018; Atkinson, 1987, Chapter 2). The tectonic history of rock can be recorded  
 362 or manifest in its brittle structures that then are maintained over a wide range of past tectonic events, including its most recent  
 363 exhumation and cooling. The attributes of resulting open or filled fractures depend on how deeply the material was buried, how  
 364 rapidly uplifted, and the material properties (e.g., English and Laubach, 2017). Finally, the fact that the current tectonic setting can  
 365 drive ongoing deformation has long been recognized (e.g., Hooke, 1972), and more recent work has highlighted that very low  
 366 magnitude tectonic stresses can translate to fracture propagation in very near-surface bedrock, especially when interacting with  
 367 local topography (e.g., Martel, 2011; Moon et al., 2020).

368  
 369 It is likely, though perhaps not widely appreciated, however, that fractures originally opened due to tectonic stresses further  
 370 propagate, not only due to ongoing tectonic stresses as they approach the surface, but also due to topographic and environmental  
 371 stresses that the rocks increasingly encounter as they are exhumed to shallower depths. Simultaneously, these ‘new’ stresses may  
 372 increase the overall number density (total number of fractures per area) and fracture intensity (defined here as total fracture length  
 373 per area). These changes in fracture characteristics may manifest abruptly with depth or more gradually and those changes may  
 374 manifest differently under different topographic portions of the landscape (ex: ridges versus valleys). There is a growing body of  
 375 data pointing to such surface interactions (e.g., Marshall et al., 2021b; Moon et al., 2019; Moon et al., 2020; St. Clair et al., 2015),  
 376 but overall, these differentiations are a topic ripe for further study.

377  
 378 Pre-existing fractures may not always be easily separable from those formed or further propagated under geomorphological  
 379 influence. Environmental stresses also produce parallel fractures (e.g., Aldred et al., 2015; Eppes et al., 2010; Mcfadden et al.,  
 380 2005), as do those related to the morphology of the eroding landscape (Leith et al., 2014). Thus, for outcrops, and particularly for  
 381 clasts where correlations or comparison with regional tectonic structures are not possible, fracture orientations may not uniquely  
 382 represent a tectonic regime. The non-geomorphic origin (or otherwise) of such fractures may be evident from microstructure  
 383 analyses that examines fractures for diagenetic cements, inconspicuous mineral deposits, fluid inclusions, or other similar features  
 384 (e.g., Ukar et al., 2019)

385 Thus, in choosing study sites, consideration should be made of rock age, tectonic history and current tectonic setting (e.g., World  
 386 Stress Map, Heidbach et al., 2018), as well as unambiguously tectonically-related structures such as dipping bedding planes,  
 387 evidence of mineral deposits in the fractures, stylolites, or ductile structures such as folds (Hancock, 1985; Laubach et al., 2019).

### 388 2.3 Bedrock outcrops versus deposited clasts

389 The fracture characteristics of outcrops have long been employed as proxies for subsurface fracture networks, and there is a  
 390 reasonably large body of literature addressing these relationships and their potential pitfalls (e.g., Ukar et al., 2019; Al-Fahmi et  
 391 al., 2020; Sharifigaliuk et al., 2021). However, as mentioned above, topographic and environmental stresses both have likely  
 392 contributed to any sub-aerially observed fracture network unless otherwise ruled out. Thus, for studies that aim to isolate fractures  
 393 associated with environmental stresses, measurements from clasts may be more useful than outcrops.

394  
 395 Clasts that have been transported by fluvial, glacial, or mass-wasting processes have experienced abrasion, and therefore, it is  
 396 highly likely that pre-existing superficial fractures have been removed. Thus, clasts may be more reasonably considered ‘fresh’  
 397 than an outcrop with an unknown exhumation history, allowing clearer linkages between environmental exposure and observed  
 398 fractures. This idea of “resetting” fractures within clasts through transport is supported by data showing clasts of identical rock  
 399 type that have experienced more transport (i.e., rounded river rocks) having higher strength than those found in, for example, recent  
 400 talus slopes (Olsen et al., 2020). Nevertheless, clasts may carry with them an invisible (to the unaided eye) population of pre-  
 401 existing fractures— or sealed microfractures—that do in some instances impart a strength anisotropy that can manifest in later  
 402 surface-related fractures, even in clasts. Thus, for such rocks, the ‘reset’ may be imperfect (e.g. Anders et al. (2014). In-depth  
 403 petrographic analysis to identify residual microstructures (e.g. ala Forstner and Laubach, 2022) may not be feasible in most  
 404 instances, but a simple uniaxial point load test, or field Schmidt-hammering of clasts found in active channels, may reveal if an  
 405 inherited anisotropy is present.

## 406 3 Selecting the clasts, outcrops, or rock surface locations that will comprise the fracture observation area

407 Carefully selecting the rock surface area(s) on which fractures will be observed and measured within a site is equally as important  
 408 as selecting the site or the fractures themselves. Hereafter, the term ‘observation area’ refers to the specific portion(s) of rock  
 409 surface(s) for which fractures are being measured. Observation areas may comprise the entire exposed surface of individual clasts,  
 410 outcrops, or portions of either (Fig. 1). In the following sections, instructions for selecting these observation areas in the field are  
 411 provided.

### 412 3.1 Establishing outcrop or clast selection criteria

413 Before observation areas can be identified, outcrops or clasts must be selected. The first step of that selection process is to establish  
 414 criteria for determining which outcrops or surface clasts within the site are acceptable for measurement. Similar to site selection,  
 415 variability in cl,o,r,p,t,T factors that may influence fracturing (temperature, moisture availability, rock shape, and rock type) should  
 416 be controlled for as much as possible.

417  
 418 In general, characteristics of the clasts or outcrops that might impact mechanical properties, moisture, or thermal stress-loading  
 419 should be most heavily considered. The rock type properties that should be considered when developing selection criteria include

420 not only heterogeneities like bedding or foliation, but also grain size and mineralogy, all of which can influence fracture rates and  
 421 style characteristics. For example, perhaps only outcrops with no visible veins or dikes will be employed; or only outcrops greater  
 422 than 1 m in height; or only north facing outcrop faces. Past work, for example, has focused on upward facing surfaces of outcrops  
 423 or large clasts (e.g., Berberich, 2020; Eppes et al., 2018).

424  
 425 For loose clasts, only clasts of a particular size or rock type might be employed for measurement. For example, past work found  
 426 that below approximately 5 cm diameter in semi-arid and arid environments (Eppes et al., 2010), and 15 cm in more temperate  
 427 environments with vegetation (Aldred et al., 2015), clasts are more likely to have been moved or disturbed. Thus, these sizes were  
 428 employed as a threshold for selection.

### 429 **3.2 Non-biased selection of clasts or outcrops for measurement**

430 Once criteria are defined, clasts or outcrops meeting those criteria must be randomly chosen for the fracture measurements. A  
 431 procedure similar to the well-vetted Wolman Pebble Count style transect (Wolman, 1954) should be employed to avoid sampling  
 432 bias. For landforms with other geometries, a grid may be used instead of a transect line.

433  
 434 In either case, a tape transect or net grid is laid out on the ground at each site, and the clast or outcrop closest to specified intervals  
 435 on the tape (or at the points of the grid meeting the criteria) is selected (Fig. 1a). The interval or grid spacing should be adjusted to  
 436 the overall size and abundance of clasts or outcrops found on the surface. If there are relatively few meeting the criteria at a site,  
 437 all within the site meeting the criteria can be measured.

438  
 439 A similar technique can and should be applied for selecting outcrops. For example, care should be taken to not be limited to the  
 440 ‘best’ outcrops (cleanest and/or largest), since they likely are the least fractured. However, such large, clean outcrops may be the  
 441 best places to observe any pre-existing subsurface-related fractures. For locations where outcrops are within a few meters or tens  
 442 of meters of each other and vegetation relatively sparse, a grid of a set dimension (e.g., 100 m) is overlain on aerial imagery, and  
 443 the closest outcrop to each grid intersection meeting the outcrop criteria are selected (Watkins et al., 2015). For areas where  
 444 outcrops are not visible in aerial imagery, a measured or paced transect can be employed where the user walks along a bearing and  
 445 chooses the closest outcrop meeting the selection criteria at each interval, e.g., 30 paces.

446  
 447 In all of the above, transect locations and orientations should be selected following consistent criteria and being mindful of the  
 448 State Factors cl,o,r,p,t,T. For example, all transects or grids might be placed uniformly along backslopes with a certain upslope  
 449 distance from the crest; or along the latitudinal center or crest of a landform. Alternatively, the transect might be orientated  
 450 perpendicular or oblique to a paleo-flow direction so that it is not constrained only to bars or swales. The coordinates and bearing  
 451 of all transects or grids should be recorded, enabling tracking and avoiding repetition.

### 452 **3.3 Observation areas comprising the entire clast or outcrop surface**

453 The observation area for small clasts and outcrops can be their entire exposed surface. When clasts or outcrops selected for  
 454 measurements are less than ~50 cm in maximum dimension, measurements can typically be readily made for all fractures visible  
 455 on the clast or outcrop exposed surface.

456  
457 No rocks should be moved during measurement. This non-disturbance practice is particularly crucial for maintaining Earth's  
458 geodiversity (Brilha et al., 2018) and preserving sites for future workers to revisit. Further, research examining acoustic emission  
459 localization of rocks naturally fracturing found that the large majority of fracture 'foci' were located in the upper hemispheres of  
460 boulders (Eppes et al., 2016). Thus, the potential insight gained by moving clasts does not warrant the impact to geoheritage.

### 461 3.4 Establishing 'windows' as the observation area for larger clasts and outcrops

462 Fractures are three-dimensional objects, and ideally observations should encompass volumes, but this is precluded by the opacity  
463 of rock, so one- or two-dimensional observation areas must be used. Fracture arrays may also encompass a wide range of sizes, so  
464 observations need to consider truncation and censoring biases, and inevitably decisions must be made about size cutoffs. Some  
465 part of the smallest size fraction of fractures may not be readily visible, and the finite size of exposures may mean that some large  
466 fractures are missed.

467  
468 When it is not feasible to measure every fracture on an outcrop or clast, the observation area may comprise predetermined  
469 'windows' of representative decimeter- to meter-scale areas of the rock surface (Fig. 1b). This window selection method results in  
470 an accurate representation of fractures on an entire outcrop (e.g., Zeeb et al., 2013) and is least affected by some subjective biases  
471 (Andrews et al., 2019).

472  
473 Importantly, the number and size of windows observed on each outcrop or at each site should depend on the typical number and  
474 size of fractures present on the surface of the rock (Sect. 4.2). Overall, it is preferable to strike a balance between window size and  
475 number so that during data analysis, variance can be quantified by comparing data collected between windows on the same outcrops  
476 and at the same site. More total observation area (e.g. more and/or larger windows) is required when fractures are fewer per area.  
477 The size of the area required for a representative quantification of fractures depends both on fracture average length and number  
478 density (e.g., Zhang, 2016). Here, an iterative approach is outlined for determining if sufficient area has been examined (Sect. 4.2),  
479 but other rules of thumb exist, particularly in the Rock Quality Designation Index literature (e.g., Zhang, 2016).

480  
481 Choosing the placement of windows on the outcrop should entail a stratified random sampling approach. Just as for clast- or  
482 outcrop-selection, cl,o,r,p,t,T factors like aspect should be taken into consideration and controlled for as much as possible in the  
483 window placement strategy by, for example, only using upward facing surfaces. Then, window placement determination is made  
484 to avoid sampling bias and edge effects. For example, if upward facing outcrop surfaces are to be characterized, then the total  
485 length and width of the face could be employed to align sufficient numbers of windows along even intervals of those measurements  
486 (e.g., three windows whose centers are located along the center axis of the rock with even spacing between the edges and each  
487 box; Fig. 1b).

488  
489 For the placement of each window, a simple cardboard template of the appropriate window size with a center hole can be employed  
490 to trace with chalk the window directly on the clast or outcrop. Then, all fracture measurements are made in the window(s). Each  
491 window should be numbered and photographed in the context of each outcrop or clast. Also recommended is detailed photo-

492 documentation of each outcrop and transect, along with sufficiently detailed coordinates to reoccupy the precise site (e.g. in meters  
493 or 0.00000 dd that are *always* referenced to the projection or datum used).

### 494 **3.5 How many observation areas?**

495 The number of clasts, outcrops, or windows required to measure sufficient fractures will vary with the study goals, site complexity,  
496 and the variables for which the data are being tested or controlled. Importantly, for each study, the required number of observation  
497 areas must be established based on the amount that is necessary to gain a statistically sufficient number of fracture observations to  
498 represent the rocks in question for that setting (Sect. 4.2). Concepts of ‘stationarity’ have been applied in the context of 2D analyses  
499 (e.g. Shakiba et al., 2023), but no rule-of-thumb in the context of surface processes is described herein because, as yet, there has  
500 not been sufficient standard fracture data collected to establish such a rule. Establishing such a rule of thumb is an illustration of  
501 the motivation of this paper, as well as an example of how the methods presented herein can and should evolve over time.

502  
503 Rocks or outcrops with lower fracture number density (fewer overall fractures per area) will require that larger areas of their surface  
504 be examined to measure sufficient fractures for statistical significance (Sects. 3.4 and 4.2). Rocks or outcrops with significant  
505 variation in fracture patterns require sufficient observation to capture that variability. Thus, as an example only, in past work, when  
506 State Factors were carefully controlled for, relationships between rock material properties and rock fracture properties were evident  
507 from about three to ten meter-scale outcrops per rock type on ridge-forming quartz rich rocks (Eppes et al., 2018). However, until  
508 sufficient magnitude of datasets have been collected for a particular site, the amount of observation area must be established based  
509 on the number of fractures available uniquely at each study site.

## 510 **4 Selecting fractures for measurement**

### 511 **4.1 Rules-based criteria for selecting fractures in surface processes research**

512 The term ‘fracture’ is employed with a wide variety of meaning across the geosciences, potentially resulting in large variations in  
513 the range of features that two individuals might study on a single outcrop (Long et al., 2019). Therefore, it is crucial to employ  
514 clear and repeatable rules-based criteria (e.g., Table 1) for what constitute measurable ‘fractures’ within any fracture-related  
515 research. Failing to do so consistently results in a high variance of subjective bias that is more reflective of worker personality than  
516 of the variance in fracture of the outcrop (Andrews et al., 2019). Thus, consistency and documentation are required for deriving  
517 interpretable and repeatable results.

518  
519 The proposed rules (Table 1) for determining which fractures to measure at any given field site were developed in the context of  
520 surface processes research and through iterations with numerous non-expert users (undergraduate students) to arrive at criteria that  
521 provided consistency in observations across users. Because surface processes are frequently and largely dependent both on rock  
522 erodibility and water within a rock body, the recommended criteria are applicable only to open voids, which are known to greatly  
523 impact both. Also, because other types of open voids like vesicles are common in rock, additional criteria includes that the open  
524 void must be planar in shape, bounded by parallel or sub-parallel sides (hereafter fracture or fracture ‘walls’), with a visible opening  
525 that is deeper than it is wide. Fracture walls will pinch together at fracture terminations.

526

527 Voids that fit the shape criteria that are filled with lichens, dust, or other permeable material that can be readily brushed out with a  
528 fingernail or prodded with a needle should be included in the dataset. However, it is common for high aspect ratio voids in rock to  
529 have been filled with cemented mineral solids during intrusion and metamorphism, diagenesis, or weathering. Fractures, or portions  
530 of fractures containing these hardened cements, may become the hydrologic and mechanical equivalent of solid rock. Fractures  
531 that are fully cemented do not meet the defined 'open' criteria and in principle should not be included in the fracture dataset. Where  
532 partly cement-filled fractures are present, specific rules may need to be adapted to account for the pattern of cement such as  
533 counting segments of fractures that are separated by continuous mineral deposits as separate features. If such a solid secondary  
534 mineral cement forms a discontinuous 'bridge' fully connecting the two walls of an otherwise open, planar void, the open length  
535 of the fractures on either side of the bridge would be treated as individual fractures. This partial 'bridge' or complete interruption  
536 of continuous fracture pore space is common in fractures that have existed at elevated temperatures such as at depth or near  
537 hydrothermal features (see review in Laubach et al., 2019), so a yes/no indication of their presence may be added to the dataset. A  
538 useful starting point for building such rules is to compare outcrops with expectations for how mineral deposits are typically  
539 configured in partly cemented fractures (e.g., Lander and Laubach, 2015).

540  
541 Finally, additional proposed criteria include that the planar void must be continuously open (no 'bridges' of cemented mineral  
542 material or of rock) for a distance longer than 10 times the characteristic grain size dimension or 2 cm, whichever is greater. In  
543 most rock types, this translates to a 2 cm minimum cutoff for countable fractures (Fig. 2a; see Sect. 5.4.1 for measuring lengths).  
544 This proposed length threshold is based on three features. First, past work has demonstrated that deriving precise (repeatable)  
545 detailed information - other than length - for fractures <2 cm in length is challenging (e.g., Eppes et al., 2010). Second, temperature-  
546 dependent acoustic emission measurements (Wang et al., 1989; Griffiths et al., 2017) and theoretical arguments suggest that on  
547 single year time scales, fractures on single grain and smaller length scales exist in thermodynamic equilibrium, randomly opening  
548 and closing under constant redistribution of ubiquitous diurnal to seasonal thermal stresses within surface rocks. The approximate  
549 statistical mechanical 'rule-of-ten' states that well-defined equilibrium and nonequilibrium, continuum-scale properties, e.g.,  
550 viscosity, density, stress and strain, each determined by myriad microscale random processes, are obtained on length scales  
551 approximately 10 times an appropriate molecular length scale, e.g., average atomic size or mean free path length between colliding  
552 (gas) molecules. This interpretation is consistent with recommendations for the number of grains the minimum diameter of a  
553 sample is for repeatable testing of continuous rock properties such as rock strength and elastic moduli (e.g., ASTM, 2017).

554  
555 Last, and practically, the high abundance of fractures below this cutoff significantly increases the time required for fracture  
556 measurement. If these smaller fractures are of interest, they can be characterized with photographic analysis (not covered herein)  
557 or subjected to semi-quantification via an index (Sect. 5.2).

558  
559 Importantly, in some applications, it may be appropriate that a larger minimum threshold in fracture length is chosen. However, in  
560 that case, fracture abundances in the rock will possibly dictate that significantly larger observation areas of the rock exposure need  
561 to be employed in order to obtain sufficient numbers of fractures to provide representative data (Sect. 4.2).

562  
563 Regardless of the threshold length chosen for the study, two adjacent fractures separated by intact rock or bridges of cement are  
564 considered two fractures, even if at a distance they appear to be continuous (Fig. 2b). This practice results in repeatable



565 measurement between multiple workers and provides the most accurate representation of past fracture growth and fracture  
566 connectivity in the rock body.

#### 567 4.2 Determining how many fractures to measure

568 Most published fracture-focused studies provide no justification for the number of fractures they measure, begging the question -  
569 is the dataset representative of the rock body? Studies of fracture statistics suggest a minimum of ~200 fractures (Baecher, 1983)  
570 per site (as defined herein). For workers and situations that require more nuance or for which there is not ample rock surface to  
571 examine, we recommend an iterative approach. It is a long-recognized concept in fracture and rock mechanics that fracture size  
572 distributions are highly skewed and can be characterized by scale-independent power law distributions (e.g., Davy et al., 2010;  
573 Hooker et al., 2014). Power law distributions cross multiple orders of magnitude in frequency and scale, requiring up to an order  
574 of magnitude more observations to significantly define than the other, more tightly defined distributions. Thus, the best practices  
575 to understand the commonly observed power-law distribution of fracture size can be leveraged in most cases to ensure that a  
576 representative fracture population has been measured in any given dataset (Ortega et al., 2006).

577  
578 Here, it is recommended that to fully characterize the fractures for any site(s), outcrop(s), or feature(s) of interest, sufficient  
579 numbers of fractures should be measured such that, if the fracture parameters are power-law distributed, a statistically robust  
580 power-law distribution (p-values <0.01) in fracture length or aperture can be estimated from the data. While other log-normal,  
581 exponential, and Weibull distributions have been proposed for various fracture datasets (e.g., Baecher, 1983), employing these  
582 distributions depends on preexisting knowledge of the expected dataset, the very data set in the process of being collected. Thus,  
583 unless there is prior documentation of fracture distributions at a particular site, the power law distribution should suffice, and, in  
584 any case, power law distributions require the most samples for significance compared to the other distributions.

585  
586 Thus, in practice, it will be an iterative process to determine the number of fractures required for any given dataset; but generally,  
587 on the order of  $10^2$  fractures are required (e.g., Zeeb et al., 2013) to reach a representative distribution (Fig. 3). When sufficient  
588 numbers of fractures have been measured to result in such a distribution, then it can be assumed that the population of measured  
589 fractures is representative of all fractures on the rock, outcrop, or group of rocks/outcrops with certain features. For example, if the  
590 goal of a study is to test the influence of rock type on fracture density, enough fractures must be measured to allow for a power-  
591 law distribution of fracture size for *each* of the rock types. That population of fractures can then be considered representative of  
592 the given rock type, and statistics on other fracture properties like width can also be reasonably interpreted as representative.

593  
594 If after ~200 fractures are measured the power law distribution is not met, then it is likely the dataset does not follow a power-law  
595 distribution and the number of measurements can be considered sufficient (Baecher, 1983). Some fracture arrays – particularly  
596 those formed at depth - have narrow (or ‘characteristic’) size distributions that are not well approximated by power laws (e.g.  
597 Hooker et al., 2013). Another exception to the scale independent power law rule of thumb may be if there are abundant fracture  
598 terminations in infilling material. In this case, the size of the fracture (as defined by Table 1) is dictated by the spacing of the filled  
599 material bridges. Thus, fracture sets in rocks that contain abundant varnish or secondary precipitates like calcium carbonate may  
600 not follow the power-law rule, and a threshold number of ~200 fractures per site should be employed.

601 An example of what the iterative process might look like is found in Fig. 3. In this example, all fractures were measured on the  
 602 surface of 15-50 cm diameter granitic clasts selected along transects across both a modern wash bar (with few overall fractures per  
 603 clast) and a ~6 ka alluvial fan bar (with many fractures per clast). For the modern wash, after 5, 30, or 50 clasts, a statistically  
 604 significant power law distribution is not evident (Fig. 3). However, after 130 clasts, the fit of the power law falls below a p-value  
 605 threshold of 0.01. Thus, measurements from around 130 clasts were necessary to fully characterize fractures for that particular site.  
 606 In contrast, the threshold p-value is reached after only 5 clasts for clasts with high fracture number density on the mid-Holocene  
 607 age site; however, with more clasts examined, more variables per clast can be analyzed in the data. Thus, in order to evaluate  
 608 different variables (like clast size or shape), the iterative process would repeat, but limiting the analysis to fractures found on clasts  
 609 meeting the criteria of interest. In this example, a total of 130 clasts per surface were measured, enabling several subsets of data to  
 610 be examined in order to test the influence on a range of clast properties on fracture characteristics. This iterative approach will give  
 611 a reasonable assurance of when enough samples have been collected, but determining the type of distribution and estimating the  
 612 distribution parameters, i.e., the exponent of the power-law, require more careful analysis that is covered below in section 6.  
 613

## 614 **5 Proposed baseline field data for fracture-focused surface processes research**

615 Here, a basic suite of field data (Table 2) is described for all observation areas and all fractures. Table 3 contains a list of  
 616 recommended field equipment to make the measurements. The list of data in Table 2 was developed with the goal of allowing the  
 617 worker to fully analyze their fracture data in the context of variables known from the literature to influence or reflect fracture in  
 618 exposed rocks. Workers may choose to measure only some of these data if, for example, they have controlled for a particular metric  
 619 through site or clast selection. As overall knowledge of fractures in surface environments grows, the suggested set of measured  
 620 variables should also change, just as, for example, the components of the simple stream power equation have evolved in fluvial  
 621 geomorphology literature. The proposed fracture field methods list is also focused on direct ‘observables’ – without interpretation  
 622 – that should apply universally across field areas. We readily acknowledge that additional items can and should be added to  
 623 accommodate the needs of any specific study.  
 624

625 The metrics listed in Table 2 and the associated methods described below are designed to be applicable and translatable to both  
 626 natural outcrops and individual clasts. While they may also be applicable to fractures found in quarries and road-cuts, such outcrops  
 627 are prone to fracturing that has been anthropogenically induced by blasting, exhumation, and new environmental exposure (e.g.,  
 628 Ramulu et al., 2009; He et al., 2012).

### 629 **5.1 The ‘Fracture Sheet’**

630 A data collection template is provided that comprises all the proposed standard data, allowing efficient, complete, and detailed  
 631 recording of all parameters while in the field (e.g., a “fracture sheet”, Fig. 4 with digital version provided in supplemental data).  
 632 The fracture sheet can and should be modified to include additional parameters relative to any study. The template provided here  
 633 is structured so that each observation area’s information (e.g., that of each clast, outcrop, or window) shares a row with the first  
 634 fracture measured. Then, subsequent rows are employed for additional measured fractures on the same observation area. Each  
 635 observation area and fracture are assigned unique identifiers to enable unambiguous reference in subsequent data analysis.

636 Employing a ‘window’ rather than an entire clast or outcrop as the observation area necessitates slightly different data collection,  
637 so two separate fracture sheets can be found in the supplement.

638

639 The fracture sheet provides a header space for site meta-data. Any observations that could elucidate the possible contributions of  
640 any State Factor (cl,o,r,p,t,T) acting at the site should be recorded (e.g., the vegetation or topography of the site). This header area  
641 should also be employed to note any and all criteria or conventions used throughout the study. For example, the use of any  
642 convention, such as right-hand rule for strike and dip measurements, should be noted in the header. The criteria employed to select  
643 clasts or outcrops (e.g., their size, composition, etc.) and the nature of the observation areas (e.g., only the north face of all clasts;  
644 or entire exposed clast surface for all outcrops) should also be noted.

## 645 5.2 The use of semi-quantitative indices

646 It is recommended that indices be employed for many observations following similar existing semi-quantitative methods  
647 commonly employed in both soil sciences (e.g., Soil Survey Staff, 1999) and sedimentology (e.g., rounding and sorting). The use  
648 of indices, rather than precise measurements, is especially appropriate for fractures and fracture characteristics given the natural  
649 variation between different rocks. Also, high numbers of small or discontinuous features on rock surfaces frequently precludes  
650 their accurate counting within a reasonable amount of time; for example, counting all fractures <2 cm in length.

651

652 Two particularly useful generic ‘abundance’ indices are defined here that are similar to those employed for quantifying the  
653 abundance of roots and pores in soils (Schoeneberger et al., 2012), whereby the quantity or coverage of specific elements or features  
654 is estimated within a specified area. For both, a ‘frame’ is employed whose size is dependent on the size of the feature being  
655 observed (Fig. 5). Features that are  $\leq 0.5$  cm are observed in 1 cm<sup>2</sup> frames; features  $>0.5$  to  $<2$  cm are observed in a 10 cm<sup>2</sup> frame;  
656 and features  $\geq 2$  cm are observed in a m<sup>2</sup> frame. Cut-out stencils of these sizes may be constructed and employed. The observer  
657 imagines randomly placing the ‘frame’ several times on any given portion of the observation area, noting the abundance of the  
658 feature of interest within the frame. The indices are based on the average value of abundance observed in any given such ‘frame’  
659 across the entire area of observation (e.g., the entire clast, the entire outcrop, or the outcrop window).

660

661 The first index scales from 0 to 4 and is applicable for ‘countable’ features of interest in the research like small fractures, fossils,  
662 or large phenocrysts. The index is: none – 0 (no visible features in any frame), few -- 1 (<1 feature on average), common -- 2 ( $\geq 1$   
663 and  $<5$  features on average), very common -- 3 ( $\geq 5$  and  $<10$  features on average), and many -- 4 ( $\geq 10$  features on average).

664

665 The second index scales from 0 to 5 and is employed for features that are not readily counted nor consistent in size (like lichen,  
666 varnish, fine grained mafic, or felsic minerals). In these cases, the index is based on the percentage of the rock surface covered by  
667 the feature: none – 0; very little – 1 (<10%); little – 2 ( $\geq 10$  and  $<30\%$ ); common – 3 ( $\geq 30$  and  $<60\%$ ); very common – ( $\geq 60$  and  
668  $<90\%$ ); and dominant – 5 ( $\geq 90\%$ ). A percentage estimator (Fig. 6) should always be employed to assign the index categories –  
669 even experienced field workers are subject to ‘quantity bias’.

## 670 5.3 Measuring rock characteristics

671 The following rock characteristics should be measured for each observation area – each clast, outcrop, and/or window – that is  
 672 employed in a study. Some fracture characteristics not captured in individual fracture measurements are also included. In particular,  
 673 fracture connectivity and fracture spacing should be measured after all individual fractures within the observation area have been  
 674 identified and measured.

### 675 5.3.1 Clast, outcrop, or window dimensions

676 Rock – or outcrop – size, aspect, and slope can impact stress-loading through, for example, thermal stress distribution (e.g., Molaro  
 677 et al., 2017; Shi, 2011). Or, for instance, natural outcrop height has been linked to its exposure age and/or erosion rates (e.g.,  
 678 Hancock and Kirwan, 2007). The dimensions of the clast, outcrop, or window employed for fracture observations are also required  
 679 for calculations of fracture number density and intensity (i.e., the number/length of fractures per unit area; see Sect. 6.1).

680  
 681 The length and width of planar ‘windows’ are measured directly. If a window ‘bends’ across multiple faces of the rock surface,  
 682 then separate length and width measurements should be made for each face with a distinct aspect. These areas are then added  
 683 together for fracture number density and intensity calculations.

684  
 685 The vast majority of rock clasts and outcrops found in nature have ‘cuboid’ forms (Domokos et al., 2020). Thus, length, width,  
 686 and height of individual clasts or outcrops may be reasonably employed to calculate the exposed surface area (see Sect. 6.1 for  
 687 calculations). If clasts or outcrops are well-rounded, spherical or half-spherical surface areas can be employed, depending on burial.

688  
 689 For all dimension measurements regardless of rock shape, metrics are measured as point-to-point orthogonal measurements. Length  
 690 is measured parallel to the longest axis. Width is measured on the widest extent that is perpendicular to length, and height is  
 691 measured vertically from the uppermost surface of the rock down to the ground surface. If a through-going fracture splits the rock  
 692 into two pieces that remain *in situ*, it should still be considered one rock and measured accordingly. If a clast or outcrop is spheroidal  
 693 in shape, that should be noted for future surface area calculations.

694  
 695 For site preservation, and to minimize geoheritage and environmental impacts, rocks should not be moved from their natural state;  
 696 therefore, the height measurement of a highly embedded rock will only represent the height of the exposed rock surface above the  
 697 ground. A metric derived to estimate the degree to which clasts are exposed versus embedded is provided in Sect. 5.3.8.

### 698 5.3.2 Sphericity and roundness

699 Sphericity and roundness from standard sedimentology practices (e.g., Krumbein and Sloss, 1951) provide metrics for rock shape.  
 700 Shape can influence stress distribution in a mass and, therefore, rock fracture. For example, generally, corners tend to concentrate  
 701 stresses, and ‘corner fractures’ are a recognized phenomenon in fracture mechanics (e.g., Kobayashi and Enetanya, 1976). Thus,  
 702 this metric has been included as one to be measured both for outcrops and for clasts.

703  
 704 Sphericity refers to the length by width ratio, or elongation, of the clast or outcrop, whereas roundness is a measure of angularity  
 705 (Fig. 7). The roundness and sphericity designation for the square on the chart in Fig. 7 most closely matching the dominant shape

706 of the entire clast or outcrop should be noted (ex. r-SR; s-SE). If a more precise rock shape analysis is needed, a modified Kirkbride  
707 device can be used to quantitatively measure rock roundness (see Cox et al., 2018 for device modifications and methodology).

### 708 5.3.3 Grain size

709 Mean grain size can impact numerous fracture and stress characteristics including the proclivity for granular disintegration  
710 (Gomez-Heras et al., 2006), fracture toughness (Zhang et al., 2018), initial fracture length, thermal stress disequilibrium (Janio De  
711 Castro Lima and Paraguassú, 2004), and bulk elastic properties (Vazquez et al., 2015). The mean grain size should be visually  
712 estimated by comparing the dominant size of individual grains or mineral crystals to a standard grain size card. This size can be  
713 reported as one average value for all minerals, or different values for different suites of minerals (e.g., felsic vs. mafic), depending  
714 on the lithological assemblage(s) of the observation area(s).

### 715 5.3.4 Fabric and fracture filling

716 Here, the term ‘fabric’ is employed to refer to any preexisting (prior to weathering) primary or diagenetic planar, linear, or randomly  
717 oriented anisotropies within the rock comprising the outcrop or clast of interest. Fabric is most commonly observed as fossils or  
718 lithological bedding planes in sedimentary rocks and as crystal horizons or foliation structures in igneous or metamorphic rocks.  
719 Also, all rocks can have diagenetic mineral deposits within parts of otherwise open fractures or contain fully filled veins and dikes.  
720 Finding mineral deposits in open fractures points to a deeper origin. Rock fabric can impart anisotropy that influences rock strength,  
721 fluid flow, and fracturing clustering, rates, and orientations (e.g., Nara and Kaneko, 2006; Zhou et al., 2022). Thus, any visible  
722 fabric type, as well as the strike(s) and dip(s) (or trend(s) and plunge(s)) of each parallel or subparallel set should be noted in the  
723 fracture sheet for each observation area. By collecting these data, it can be determined by comparing orientations the extent  
724 fractures in the dataset are influenced by these fabrics.

### 725 5.3.5 Fractures <2 cm in length

726 Fractures <2 cm in length can comprise a significant portion of all fractures on a given rock exposure, particularly in coarse  
727 crystalline rock types (e.g., Alneasan and Behnia, 2021). Thus, it is recommended that an index is recorded, using an observation  
728 ‘frame’ (see Sect. 5.2) that quantifies the abundance of fractures less than 2 cm in length (hereafter ‘small fractures’).

729  
730 The approximate number of small fractures visible each time the ‘frame’ is moved should be observed. A rough average of all  
731 theoretical frames should be taken, and the categories in Fig. 5 should be used to assign an abundance. For example, if there are  
732 generally either zero or one small fracture in any given 10 x 10 cm frame, the abundance would be “1” – i.e., few, <1 per unit area.

### 733 5.3.6 Granular disintegration

734 Granular disintegration refers to evidence of *active* loss of individual crystals or grains due to fracturing along grain boundaries  
735 (i.e., sedimentary particles or igneous or metamorphic crystals). This feature is observed on the rock surface as individual grains  
736 or small clusters of grains of the rock that can be brushed away by hand. Granular disintegration is commonly observed in coarse  
737 igneous, metamorphic, and sedimentary rocks, and over the long-term leads to the accumulation of ‘grus’ - sediment comprised of  
738 individual crystals or small clusters of a few crystals on the ground surface (Eppes and Griffing, 2010; Isherwood and Street, 1976;  
739 Gomez-Heras et al., 2006).

740

741 This disintegration comprises the complete separation of intergranular fractures. Because the fractures that comprise granular  
 742 disintegration are typically too small to be readily measured in the field, however, its presence is assumed when loose grains are  
 743 present on the rock surface. The worker should mark affirmatively (circling the ‘G’ on the Fracture Sheet) if there is evidence of  
 744 granular disintegration on the rock surface of observation. If more detail is desired, an abundance index (e.g., Fig. 5) may be  
 745 employed to quantify what percentage of the surface of observation contains loose grains.

### 746 5.3.7 Pitting

747 Pitting is the occurrence of small holes or fissures that form on the rock surface due to granular disintegration or to preferential  
 748 chemical weathering of certain mineral types, typically feldspars and micas in silicate rocks. Pitting is distinct from granular  
 749 disintegration as it is not necessarily ‘actively’ occurring – i.e., pitting can exist without loose grains on the rock surface. It is  
 750 included here as a rock property because of its possible linkage to intergranular fracturing. Furthermore, measuring the extent and  
 751 depth of pitting due to chemical weathering has long been employed as a relative age dating tool in Quaternary geology applications  
 752 (Burke and Birkeland, 1979).

753

754 Pitted surfaces form as individual grains become weathered and fall out or are dissolved; or, for soluble rocks like carbonates, as  
 755 entire rock regions are dissolved. Pitting can either be quantified as present/absent (circling P on the fracture sheet) or as a quantity  
 756 index (Figs. 4 and 5).

### 757 5.3.8 Clast exposure

758 This metric is used to record to what degree individual clasts appear to be exposed above the ground surface. Individual clasts are  
 759 known to weather and erode from the upper rock surface down until they become ‘flat’ rocks at the ground surface (e.g. Ollier,  
 760 1984). Surface exposure can be estimated as the amount and shape of a boulder’s exposed surface that is currently not covered by  
 761 loose sediment, vegetation, or other material. This exposure is grouped into four categories: 0 - the clast is sitting above the ground,  
 762 and its sides curve downward toward the ground surface almost meeting; 1 - the clast is partially covered, with sides curving  
 763 downward toward the ground surface but not meeting; 2 - the clast is “half” covered, with sides projecting roughly vertically into  
 764 the ground surface; 3 - the clast has only one upward facing side visible at the ground surface. In a field study, a correlation test  
 765 on data from 300 boulders revealed a positive correlation of 0.66 between the indices and the fraction of boulder embeddedness  
 766 (in vertical length) (Shaanan et al., 2022).

### 767 5.3.9 Lichen and varnish

768 Lichens and other plant life can act to push rocks apart during growth (Scarciglia et al., 2012), but have also been shown to  
 769 strengthen rocks through infilling of voids or shielding from stress-inducing sunlight (Coombes et al., 2018). It is noted that lichen  
 770 are living organisms that would be killed by removal. In order to determine if a lichen-coated lineation is in fact a measurable  
 771 fracture (see Sect. 4.1), a needle or straight pin may be employed to poke through the lichen into the possible void of the fracture.

772

773 Rock varnish (oxide staining that can appear as a dark gray/black or orange coating on rock and typically contains Fe or Mn oxides)  
 774 is well-documented to evolve over time. The extent of varnish cover has been employed frequently as a relative-age indicator,

775 particularly in arid environments (e.g., Mcfadden and Hendricks, 1985; Macholdt et al., 2018). Thus, variations in varnish across  
 776 the rock face can provide evidence of loss of surface material through *in situ* fracturing.

777

778 Lichen and varnish can come in many forms and be difficult to distinguish from each other and from primary rock minerals, hiding  
 779 in fractures, pitting holes, and atop mafic crystals. So, careful consideration of the types of lichen and varnish that may be found  
 780 in field sites and close inspection with a hand lens is recommended. A fresher exposure of the rock surface can help in the  
 781 identification of lichen and varnish relative to the natural rock composition and color. Due to the geodiversity impact, however,  
 782 such exposures should not be made with force.

783

784 The quantity of lichen and varnish (secondary chemical precipitates deposited on the subaerial rock surface) visible on the rock  
 785 observation surface are separately estimated using a visual percentage estimator (Fig. 6) and a quantity index is assigned (Fig. 5;  
 786 Sect. 5.2).

787

#### 788 5.3.10 Collecting samples for microfracture analyses

789 Rock microfractures (those not visible with hand lens in the field) play a central role in contributing to rock strength, anisotropy,  
 790 and subsequent macrofracturing processes (Kranz, 1983; Anders et al., 2014). It is beyond the scope of the field-based methods  
 791 presented herein to describe microfracture measurement and analysis, which continues to evolve (e.g., Griffiths et al., 2017; Healy  
 792 et al., 2017). Instead, suggestions for rock sampling and placement of thin-section billets are provided.

793

794 Thin-section analysis of microfractures can be a time-consuming process, particularly when considering the per-capita rock volume  
 795 examined. It is therefore extremely important to select rock or portions of rock that are precisely the rock type of interest, and to  
 796 carefully orient the sample. For loose clasts, an entire clast can be sampled and a thin-section billet processed in the lab. For larger  
 797 clasts and bedrock, a smaller portion must be extracted. By sampling pieces that are already naturally detached, or nearly detached,  
 798 fracturing that arises due to chiseling or hammering is avoided. Epoxying samples prior to thin section preparation helps preserve  
 799 delicate features and avoids introducing artifacts. Extra-thick sections are recommended for microfracture work, since conventional  
 800 sections are prone to develop fractures during grinding. For population sampling, continuous sections can be created of any length  
 801 (Gomez and Laubach, 2006).

802

803 For both clasts and outcrops, the natural orientation of the sampled rock (its horizontal and azimuthal directions) should always be  
 804 marked on the specimen. The sample should be photographed prior to removing from its location. It is essential to ensure all  
 805 permitting is in place prior to sampling.

806

807 Similar to clast or outcrop selection, care must be taken when considering the location within the rock that the thin-section billet  
 808 will be cut. Because microfracture strike and dip can be influenced by environmental, gravitational, and tectonic forces, both the  
 809 depth and orientation of the billet should be noted and controlled for as appropriate for all samples compared within a single study.

#### 810 5.3.11 Fracture connectivity

811 Fracture connectivity refers to the arrangement of fractures relative to each other and has long been recognized as being key to  
 812 rock strength and fluid flow (e.g., Rossen et al., 2000; Long and Witherspoon, 1985; Manzocchi, 2002; Viswanathan et al., 2022),  
 813 and presumably contributes to rock erodibility given that fractures must intersect for rock to erode. There is a large body of literature  
 814 that addresses fracture connectivity and how to measure it (e.g., Berkowitz, 2002; Barton et al., 1993; Healy et al., 2017; Sanderson  
 815 and Nixon, 2018), especially in the context of reservoirs and rock quality index studies. As yet, fracture connectivity has been little  
 816 studied in the context of surface processes, but likely holds high potential given its relationship to water access and to erodibility.  
 817 Here, the focus is on a simple, rules-based observation of fracture intersection ‘nodes’ (e.g., Barton and Hsieh, 1989; Manzocchi,  
 818 2002; Forstner and Laubach, 2022; Sanderson and Nixon, 2018) that comprise the basis for fracture network connectivity  
 819 assessment (e.g., Andresen et al., 2013).

820

821 After all fractures within each observation area have been identified and measured (Sect. 5.4), all fracture links within the  
 822 observation area should be counted and recorded by noting their relationship to other fractures (Fig. 8): dead end (I-node),  
 823 crossing (X-node), and/or abutting without crossing (Y-node). Numbers of nodes per area can then be used as a proxy for  
 824 fracture connectivity. If fracture connectivity is of particular interest for the research, rules-based ‘contingent mode’ (C-node)  
 825 intersections may also be added (Forstner and Laubach, 2022). An example of a C-node rule might be if fractures >100 mm in  
 826 length terminate within 10 mm of another fracture, its termination would be a c-node. Another C-node definition could comprise  
 827 intersection relations where visible connected traces are sealed with secondary minerals. These c-nodes may be important when  
 828 there are ambiguous at-depth relationships between fracture terminations (e.g., Fig. 2b).

829

### 830 5.3.12 Fracture spatial arrangement

831 In addition to overall fracture density, intensity and connectivity, the arrangement of fractures in space (e.g., evenly spaced,  
 832 random, clustered in space) can impact loci of rock mass weakness, fluid flow, and landscape morphology. Laubach et al. (2018)  
 833 comprises a special issue of the Journal of Structural Geology devoted to spatial arrangement of fractures, and much work has been  
 834 published since. The mathematical analysis of spatial arrangement and rigorous identification of clustering is beyond the scope of  
 835 this field guide. Freely available software is available for analyzing one-dimensional fracture arrangement along scan lines (Marrett  
 836 et al., 2018) and for analysis of trace patterns in two dimensions (Corrêa et al., 2022; Shakiba et al., 2022).

837

838 For scanline-based methods, following similar methods as those used for locating windows (Sect. 3.4),  
 839 lines should be established across representative parts or the center an observation area. For 1D analysis,  
 840 good practice is to establish at least two perpendicular lines to capture different orientations of fractures,  
 841 but the optimal number and configuration depends on the pattern under investigation. A tape or other linear  
 842 measuring tool is then arranged along the lines, and, beginning with the edge of the observation area as  
 843 distance 0, the distance along the tape of each fracture is noted (in other words, the sequence of **spacing**  
 844 **between** fractures is recorded), with each measurement linked to the “Crack ID” already established for that  
 845 fracture on the Fracture Sheet. If fractures are **already** marked with chalk, this is an easy process. In that  
 846 way, the size of each fracture and its adjacent distances are noted (analysis procedures allow weighting by



847 fracture height, length, or aperture). As with any measure of fracture aggregate properties such as intensity  
 848 or connectivity, for fractures having a wide range of sizes, arrangement results depend on the size range of  
 849 fractures included in the analysis (scale dependent) (e.g. Ortega et al., 2006). These spatial arrangement  
 850 data can go on the back of the Fracture Sheet.

#### 851 5.4 Individual fracture characteristics

852 The following properties are measured for each fracture found within the observation area that meets all the fracture selection  
 853 criteria listed in Table 1. In order to keep track, it is useful to mark fractures with chalk within the observation area after you  
 854 have made their appropriate measurements.

##### 855 5.4.1 Length

856 Fracture length is measured for the entire surface exposure length of the fracture; i.e., around corners and up and down rock  
 857 topography (Fig. 2a). Measurements can be made with flexible seamstress tape to follow the curve of a fracture's exposure on the  
 858 rock surface. Length is only measured where there is an open void (Fig. 2b; Sect. 4.1), because to measure across bridges of  
 859 secondary cemented material or rock would be to infer future fracture propagation that has not yet occurred. By only measuring  
 860 the open portion of voids, the user avoids arbitrary interpretation of possible behavior. Thus, if a seemingly continuous fracture  
 861 (Fig. 2b, left inset) is in fact separated by bridges of solid rock (Fig. 2b, right inset), then these should be measured as two different  
 862 fractures and their lengths should terminate at the rock bridges. The inset in Fig. 2b reveals four fractures possibly meeting all  
 863 Table 1 criteria. If two fractures intersect in x- or y-nodes (Fig. 8), each fracture is defined by its own distinct strike, and the full  
 864 length of the full open fracture with that strike is measured (e.g., the length of segments ab and cd in Fig. 8).

865  
 866 Importantly, when using a 'window' approach to rock observation area, both the total length of the fracture extending beyond the  
 867 window, as well as the total length within the window, should both be recorded. The latter is employed in fracture intensity  
 868 calculations (Sect. 6.1); the former provides representative information about all fracture lengths on the rock being measured.

##### 869 5.4.2 Width

870 Fracture aperture widths (hereafter, 'widths') can impact both the strength and permeability of rock. Generally, they scale with  
 871 fracture length and, thus, can possibly reflect the innate subcritical cracking parameters of the rock (Olson, 2004). Fracture widths  
 872 typically vary along their exposure and pinch out at fracture tips. Determining an average or representative width within a single  
 873 fracture can thus be somewhat arbitrary and subject to bias. Locating the widest aperture is less subject to bias and can also provide  
 874 information about fracturing processes (for example, the widest aperture in a series of mechanically interacting en echelon fractures  
 875 should be in the center fracture). Also, the center of the open fracture is an objectively repeatable location, and also where the  
 876 fracture might be expected mechanistically to be the widest. However, given that this relationship can become complicated as  
 877 fractures fill or branch, it is recommended here to record fracture width both at the midpoint of the measured length of the exposed  
 878 fracture as well as at its maximum width along its exposure.

879

880 Both measurements should only be made in regions of the fracture where fracture walls are parallel or sub-parallel (e.g., green  
 881 arrows in Fig. 9), avoiding locations where fracture edges have been obviously rounded by erosion or chemical weathering, or  
 882 where large pieces have been chipped off or are missing (e.g., red arrows in Fig. 9). If it is unclear if a portion of the fracture has  
 883 chipped off (e.g., orange arrow in Fig. 9), a notation can be made and employed later to eliminate potential outliers in the dataset.  
 884 Fractures greater than about 3 mm in width can be easily measured by inserting the back-blades of digital calipers into the widest  
 885 opening of the fracture. For narrower fractures, a logarithmically binned ‘crack comparator’ (Fig. 7) is recommended (Ortega et  
 886 al., 2006), whereby the line on the comparator most closely matching the fracture aperture is chosen.

### 887 5.4.3 Strike and dip

888 Fracture orientation (i.e., strike and dip) is a function of the orientation of existing anisotropy within the rock and the orientation  
 889 of the principle stresses that drove its propagation. Fracture orientations are commonly related to tectonic forces; however, both  
 890 gravitational and environmental stresses can also be directional (e.g., St. Clair et al., 2015; Mcfadden et al., 2005). When fractures  
 891 are growing at subcritical rates, they can lengthen through a series of ‘jumps’ that link parallel or subparallel smaller fractures. The  
 892 following suggestions are for research aimed, not at characterizing these small mm-cm scale heterogeneities, but rather identifying  
 893 major stresses and heterogeneity in the entire rock body.

894  
 895 Fracture orientation is measured with a geological compass or similar tool that has both azimuthal direction and inclinometer  
 896 functionality. When measuring strike and dip of fractures, it is important to visualize how the fracture plane intersects the rock  
 897 surface, as if slipping a sheet of paper into the ‘file folder’ of the fracture. For larger fractures, weathering and erosion may have  
 898 resulted in loss of rock along the upper edge of the fracture, so it is imperative to measure the angle at the interior of the fracture  
 899 where its walls are parallel (Fig. 9) to avoid measuring instead the angle of the eroded face.

900  
 901 Fractures grow until they intersect other fractures and/or branch segment and link. If fractures appear to intersect, branch or link  
 902 (i.e., two connected planar voids with noticeably different orientations joined by a sharp angle), their lengths should be measured  
 903 separately as well as their orientations (e.g., two strikes and dips) as previously mentioned. This phenomenon is in some cases  
 904 evident in 2D spatial analysis that takes length scales into account (e.g., Corrêa et al., 2022). For fractures that meander around  
 905 mm-cm scale heterogeneities like phenocrysts or fossils, the overall trend is measured. A 1 to 10 rule of thumb can be used whereby,  
 906 as long as the ‘jog’ in the fracture orientation is  $<1/10$  of the fracture length, it is not measured.

907  
 908 Fracture tip propagation direction may also slowly change as the orientation of external stresses or internal stress concentrations  
 909 change within the rock mass. For curvilinear fractures, the average orientation can be measured, as the orientation of the non-  
 910 curved plane whose ends are defined by the ends of the fracture. Alternatively, the fracture curvilinear plane may be subdivided  
 911 into roughly linear planes and each orientation measured. If this latter approach is taken, the intersection should be marked as a  
 912 node, and two lengths recorded. It is important to note which method was employed and to remain consistent for all measurements.

913  
 914 There are numerous commonly-employed conventions for measurements of strike and dip. If the worker is consistent and clear in  
 915 the use of their preferred convention and in the presentation of their data, any are acceptable. If the worker has no such prior habits,  
 916 record strikes as an azimuthal orientation from 0-359 degrees, and dip angle as an angle deviation from horizontal of 0-90 degrees.

917 For dip direction, a convention such as the “right-hand rule” should be employed whereby the dip direction is always known from  
 918 the orientation of the strike alone. For example, the right-hand rule states that the down-dip direction is always to the “right” of the  
 919 measured and recorded strike when the observer is facing the same direction of the strike. Therefore, the strike that is recorded is  
 920 the one whereby the dip direction is always +90 degrees clockwise (to the right) from the strike direction.

#### 921 5.4.4 Fracture parallelism

922 Noting the parallelism of the fractures can help to better understand the origins of the population of fractures at a site. Parallelism  
 923 is common because fractures often follow rock heterogeneities or anisotropies such as bedding, foliation, veins, or even the rock  
 924 surface. Fractures in a single bedrock outcrop or clast are also commonly parallel because they have formed due to external stress-  
 925 loading with a consistent orientation (e.g., those influenced by regional tectonics or directional insolation). Thus, noting parallelism  
 926 may help to distinguish the origins of fractures, though not always. For example, ‘surface parallel fractures’ (e.g., Fig. 2a) -  
 927 commonly referred to as exfoliation, sheeting joints (e.g., Martel, 2017), or spalling – vary dramatically in scale and can have  
 928 origins related to several different factors including tectonic-topographic interactions (Martel, 2006), chemical weathering and  
 929 volumetric expansion (Røyne et al., 2008), and thermal stresses related to insolation (e.g., Lamp et al., 2017; Collins and Stock,  
 930 2016) and fire (e.g., Buckman et al., 2021). Likewise, fractures having a strong preferred orientation parallel to topographic features  
 931 like escarpments or stream channels may predate the topography and have localized the geomorphic feature, or they may postdate  
 932 the feature and themselves be a response to topographic loads. For this reason, fracture pattern sampling that seeks to avoid or  
 933 characterize these effects should include exposures distant from such ambiguous situations (i.e., close to and distant from  
 934 topographic features).

935  
 936 In the fracture sheet, features to which the fracture is parallel should be documented. A visual inspection will suffice for most  
 937 applications, but for applications where more precision is needed, the fracture may be considered parallel if the strike and dip of a  
 938 fracture is within  $\pm 10^\circ$  of the orientation of the feature (the rock’s long axis, its fabric, or its outer surface). A fracture may be  
 939 parallel to more than one feature in the rock. Categories may be added as necessary for rocks with other repeating features unique  
 940 to the field site (fossils; veins, etc.). Assertions of parallelism (or similar) are a potential source of ambiguity, so careful consistency  
 941 in the quantification of the basis of the claim is needed.

#### 942 5.4.5 Sheet height

943 Surface parallel fractures naturally detach ‘sheets’ of rock between the fracture and the rock surface (‘h’ in Fig. 2a). The thickness  
 944 of these sheets may be of interest for understanding the size of sediment produced from the fracture or for understanding the  
 945 stresses that produced the fracture. Sheet height is measured using calipers at the location of the maximum height of the sheet and  
 946 is only used for surface parallel fractures. To limit these measurements to those that have likely formed in situ as related to the  
 947 current morphology of the rock, a rule of thumb is to only measure those ‘sheets’ that would result in removal of <10% from the  
 948 outer surface of the rock downward into the dimension(s) of the rock face(s) to which they are perpendicular.

#### 949 5.4.6 Weathering index

950 Rock fracture is ultimately a molecular scale bond-breaking process; so, when fractures propagate, they initially form a razor-sharp  
 951 lip or edge where their two planes intersect the rock surface. Over time, these edges naturally round through subsequent chemical

952 and physical weathering, erosion, and abrasion (e.g., regions of the red arrows in Fig. 9). Crack tips may also blunt through time,  
 953 but that observation may be complicated by the presence of mineral deposits. Following similar research that has demonstrated  
 954 time-dependent changes in rock surface morphology due to such weathering processes (e.g., Shobe et al., 2017; Gómez-Pujol et  
 955 al., 2006; McCarroll, 1991), we established an index of relative degree of such rounding along a fracture edge (rather than crack  
 956 tip) to be noted in the fracture sheet:

- 957  
 958 1: fresh with evidence of recent rupture (flakes/pieces still present, but not attached)  
 959 2: sharp, no rounded edges anywhere  
 960 3: mostly sharp with occasional rounded edges  
 961 4: mostly rounded edges with occasional sharp edges  
 962 5: all rounded edges  
 963

## 964 6 Suggestions for data analyses

965 When the data collection has been completed, it is necessary to provide statistics. For initial data exploration, general properties  
 966 may be calculated for rock and fracture data like the mean, median, variance, skewness, kurtosis, and overall ‘appearance’ of  
 967 distributions. Data can be compared using normal cross-plots, or quantile-quantile plots, as well as standard correlation analysis.  
 968 For categorical data, normal analytical techniques (histograms, discrete correlation analysis, etc.) can be applied. As with all heavy-  
 969 tailed data, the median is preferred over the mean value to understand a characteristic value—though power distributed data  
 970 generally does not have a characteristic dimension. 2D spatial analysis methods can also be applied to entire outcrops or clasts, or  
 971 to subdivisions of these features (Corrêa, et al., 2022; Shakiba et al., 2023). These methods are well suited to large outcrops and  
 972 well exposed fracture arrays.

973 For the fractures themselves, the type of distribution for the fracture data can be determined and provide important insights. Not  
 974 all observations of fracture characteristics will be power-law distributed, with other heavy-tailed distributions possibly indicating  
 975 other, less random controls on fracture properties; this is quite technical, and the reader is referred to Clauset et al (2009). If the  
 976 data set is power-law distributed, then the power law exponent – the slope of the distribution in log-log plots—is the key parameter  
 977 that determines the distribution of different fracture geometries. While it is tempting to just plot the data on a log-log plot and fit a  
 978 line, this approach has proven to produce incorrect, strongly biased estimate. Again, without performing correct, unbiased statistical  
 979 analysis, it is not possible to compare the power-law behavior and other statistics between different, carefully, and time-intensively  
 980 collected data sets, limiting how generalizable the results are. Two straightforward, alternative approaches are described below.

981 To understand fracture length and fracture width data, it is key to first recognize that, with the exception of studies such as in rocks  
 982 with fractures with uniform spacing and bedding-controlled widths (Ortega et al., 2006), the data will commonly have a heavy-  
 983 tailed distribution, such as lognormal, gamma, or power law. As mentioned above, of these, strong observational and theoretical  
 984 evidence suggests that fracture size is most commonly power law distributed (e.g., Bonnet et al., 2001; Davy et al., 2010; Hooker  
 985 et al., 2014; Ortega et al., 2006; Zeeb et al., 2013), i.e.,

$$986 \quad n(b) = Ab^{-\alpha} \quad (1)$$

987 where  $b$  is the fracture dimension (length or width) of interest,  $n$  is the number of fractures with dimension  $d$ , and  $A$  and  $\alpha$  are  
 988 constants. When log-transformed, Eq. (1) becomes

$$989 \quad \mathbf{log}(n(b)) = \mathbf{log}(A) - \alpha \mathbf{log}(b) \quad (2)$$

990 which has led many practitioners to fit Eq. (2) by linearly binning the data in  $n$ , then log-transforming the data and fitting the  
 991 resulting data with a linear regression. This has proven to lead to significant bias in estimates,  $\hat{\alpha}$ , of the power law exponent  
 992 (Bonnet et al., 2001; Clauset et al., 2009; Hooker et al., 2014) and is not recommended despite its common usage.

993 Two straight-forward approaches have been shown not to have biases, or misestimates of the exponent  $\alpha$ . 1) The following is based  
 994 on Clauset et al. (2009). First, the exponent can be found from the cumulative distribution of the dimensions,  $C(b)$ , or number of  
 995 fractures with dimension greater than  $b$ , i.e.,

$$996 \quad C(b) = \int_b^{b_{\max}} n(b) db \quad (3)$$

997 Where  $b_{\max}$  is the maximum size of the fracture dimension (e.g., maximum length or width). The cumulative power law distribution  
 998 has the form

$$999 \quad C(b) \propto b^{1-\alpha} \quad (4)$$

1000 It is common to denote  $1-\alpha$  as  $c$ . To find  $\alpha$  (or  $c$ ), the dimension data is logarithmically binned. In other words, the dimension data  
 1001 is binned on a logarithmic (1, 10, 100, ...) frequency scale, and then log-transformed. At this point, linear regression techniques  
 1002 can be applied to estimate  $\alpha$  and assess uncertainty. However, in all cases, uncertainty estimates such as  $R^2$  will overestimate the  
 1003 certainty for such log-transformed data; but at least the estimate of  $\alpha$  is unbiased.

1004 2) Another method to find  $\alpha$  from a data set of fracture dimensions is to use the maximum likelihood estimator (MLE) given by

$$1005 \quad \hat{\alpha} = 1 + N \left[ \sum_{i=1}^N \ln \left( \frac{b_i}{b_{\min}} \right) \right]^{-1} \quad (5)$$

1006 where  $\hat{\alpha}$  is the estimate of the exponent in (1),  $b_i$  is the dimension of the  $i$ th fracture,  $b_{\min}$  is the minimum valid fracture dimension  
 1007 (see below) and  $N$  is the total number of samples (Clauset et al., 2009; Hooker et al., 2014). The MLE estimate has the advantage  
 1008 of an accurate estimate of standard error,  $\sigma$ , given by

$$1009 \quad \sigma = \frac{\hat{\alpha}-1}{N} + \mathcal{O}\left(\frac{1}{N}\right). \quad (6)$$

1010 Clauset et al. (2009) showed that both the logarithmically-binned cumulative distribution and the MLE estimator produce unbiased  
 1011 estimates of the exponent. For all empirical power law distributions, there is a scale; in this case  $b_{\min}$ , below which power law  
 1012 behavior is not valid. This can be visually assessed by plotting Eq. 2 with logarithmically binned  $n$ . The interval between  $b_{\min}$  and  
 1013  $b_{\max}$  where the slope is linear is where the power law is valid (Clauset et al., 2009; Ortega et al., 2006), and Clauset et al. (2009)  
 1014 presents a formal method to find  $b_{\min}$  and  $b_{\max}$ . Hooker et al. (2014) use a  $\chi^2$  test to evaluate the goodness of fit, which is simpler  
 1015 than the  $p$ -tests of the Kolmogorov-Smirnov statistic proposed by Clauset et al. (2009).

## 6.1 Fracture number density and fracture intensity

Here, following large portion of fracture mechanics literature and for clarity, the term ‘fracture number density’ is employed to refer to the number of fractures per unit area (e.g., # fractures/m<sup>2</sup>), and the term ‘fracture intensity’ to the sum length of all fractures per unit area (e.g., cm/m<sup>2</sup>). However, it is crucial to note that these terms are frequently defined differently and in inconsistent ways across disciplines and even within disciplines (e.g., Barthélémy et al., 2009; Narr and Lerche, 1984; Ortega et al., 2006; Dershowitz and Herda, 1992). It is imperative that workers clearly define their usage in each work. In particular, fracture intensity is scale dependent. If the outcrops or clasts on which fractures are measured vary greatly in size, intensity calculations that account for the fracture distribution may be appropriate (e.g. Ortega et al., 2006).

In the suggested simple use herein, the ‘area’ refers to the surface area of observation area. For fractures measured in ‘windows’ (Sect. 3.4), the length of fractures only *within* the window is used, and the area of the window (e.g., 10 cm x 10 cm) for the calculations. For loose clasts and outcrops, the appropriate calculation of surface area will depend on the shape and angularity of the rock. For most rocks, calculations for the surface area of the exposed sides of a rectangular cuboid ( $L*W + 2*(L*H) + 2*(W*H)$ ) are appropriate.

## 6.2 Circular data

Standard ‘linear’ statistics cannot be employed for circular data. Instead, circular statistical and plotting software can be used for the visualization and analysis of strike and dip data. The statistics employed by such software is typically based on established circular statistical research methods (e.g., Mardia and Jupp, 1972; Fisher, 1993). The following statistics are useful in reporting strike and dip data.

The Mean Resultant Direction (a.k.a. vector mean, mean vector) is analogous to the slope in a linear regression. Circular variance can be quantified using either a Rayleigh Uniformity Test (for single mode datasets) or a Rao Spacing Test (for datasets with multiple modes), whereby p-values <0.05 indicate non-random orientations. If p-values for these tests are below a threshold (e.g., <0.05), then data are considered non-uniform or non-random.

The Rayleigh statistic is based on a von Mises distribution (i.e., a normal distribution for circular data) of data about a single mean (i.e., unimodal data). Therefore, for multi-modal data, the variance might be high, but nevertheless, the data might be non-uniform. The Rayleigh Uniformity Test calculates the probability of the null hypothesis that the data are distributed in a uniform manner. Again, this test is based on statistical parameters that assume that the data are clustered about a single mean.

Rao's Spacing Test is also a test for the null hypothesis that the data are uniformly distributed; however, the Rao statistic examines the spacing between adjacent points to see if they are roughly equal (random with a spacing of  $360/n$ ) around the circle. Thus, Rao's Spacing Test is appropriate for multi-modal data and may find statistical significance where other tests do not.

## 8 Case example

Here we present a simple, brief example of how the presented methods promote consistency of results across users in fracture measurements; to provide a full case study is beyond the scope of this work. We provided minimal training (one demonstration

with some minor oversight of initial work) to four groups of two students each. The fifth pair of workers included a scientist who had logged over 500+ hours of experience using the standardized methods. Each of the five groups followed the methods to measure the length and abundance of fractures on boulders (15-50 cm max diameter) on the same geomorphic surface (a 6000-year-old alluvial fan in Owens Valley California, comprised of primarily granitic rock types). Each group followed the methods described herein for rock and fracture selection and measurements. As such, the results from each group (Fig. 10; Data Supplement) could be compared not only for fracture selection and measurements, but also for observation area selection – a key component of collecting data that is representative of a particular site.

We find that the data collected by each of the groups for fracture length, number of fractures per rock, and rock size are statistically indistinguishable by student t-test (all pairs of p-values > 0.1; Fig. 10; Data Supplement). Also, there is no consistent difference between measurements made by the novice groups and that of the trained group. The mean fracture lengths from the four novice groups (37±23 mm to 59±51 mm) span across that of the mean collected by the well-trained group (42±22 mm; Supplement), as do the number of fractures per rock (2±2 to 6±8 for novice groups compared to 3±3 for trained group). With only one exception (fracture length for Group 1), variance between groups does not range by more than a factor of 3 in any of the data – a common rule of thumb for the threshold of ‘similar’ variance between small datasets. Overall, especially given the relatively small size of the datasets (~10-20 rocks and ~40-60 fractures each), this comparison suggests that the results using the standardized methods are reproducible, even with novice workers with minimal training. A full case study and analysis would be required to fully and quantitatively evaluate all of the procedures presented herein.

## 9 Conclusions

The methods proposed herein comprise a ‘first stab’ at standardization of field data collected in rock fracture research surrounding surface processes and weathering-based geologic problems. The outlined methods comprise best practices derived in large part from existing work in the context of structural geology and geotechnical engineering. They also comprise general guidance and nuances developed from experiences (and mistakes) over the last two decades of fracture-focused field research applied to geomorphology and soil science. We readily acknowledge that additional, fewer, or altered methods may be appropriate for some applications. Nevertheless, it is our hope that providing these rules-based, detailed, accessible, standardized procedures for gathering and reporting field-based fracture data will open the door to rapidly building a rigorous galaxy of new datasets as these guidelines and methods become more widely adopted. In turn, they may enable future workers to better compare and merge fracture data across a wide range of studies. Doing so will permit future refinements not only of the methods themselves, but most importantly of our understanding of rock fracture. Compiling such a standardized global dataset is the best hope for fully characterizing the role and nature of fractures in Earth surface systems and processes.

## 10 Author Contributions

MCE spearheaded the evolution of the development of the guiding principles and methods described herein as well as writing of the manuscript. AR and SL contributed significantly to the editing of the manuscript’s content and expanding the breadth and depth of its applicability and approaches. JA, SB, MD, SE, FM, SP, MR, and US all participated extensively in field campaigns during which the methods were developed and refined, and they contributed to editing of manuscript and editing and development of

1087 figures. MM, AR and RK contributed to the development of theoretical statistical analyses practices that are outlined in the  
1088 document and the editing of the manuscript.

### 1089 **11 Competing interests**

1090 The authors declare that they have no conflict of interest.

1091

### 1092 **12 Data Availability**

1093

1094 All data presented in the manuscript are available in the Supplement.

### 1095 **13 Acknowledgements**

1096 The body of knowledge presented herein was derived in large part over the course of research funded by the National Science  
1097 Foundation Grant Nos. EAR#0844335 (with supplements #844401, #0705277), #1744864, and NSF-BSF #1839148 and NASA  
1098 ROSES Mars Data Analysis Program award #NNX09AI43G. Several photographs in figures were cropped and employed with  
1099 permission from Marek Ranis, Artist-in-Residence for NSF #1744864. We thank Claire Bossennec and Colin Stark for their  
1100 constructive reviews. In addition, the authors wish to acknowledge the contributions from countless undergraduate and graduate  
1101 students who contributed to the application and development of these methods in classes taught by MCE at the University of North  
1102 Carolina at Charlotte.

1103

1104

1105



## Figure Captions

Fig. 1. Images illustrating the selection of observation areas for clasts and outcrops. A. Photograph of a transect established for clast selection. Black dot: predefined transect interval location on the tape. Red dot: clast that does not fit the predefined clast selection criteria (e.g., it is too big). Green dot with red circle: clast that fits criteria but is further away from the interval point than the clast with the green dot. Green dot: closest clast to the transect interval that meets the selection criteria. B. Annotated photograph showing an idealized placement of ‘windows’ (dashed black squares) on a bedrock outcrop. Outcrop dimensions are measured and the windows are placed using predetermined selection criteria. In this example, the windows are equally spaced along the centerline of the long-dimension of the upward-facing side of the outcrop.

Fig. 2. A. Example of the measurement of a surface exposure length (L; yellow line) of a fracture meeting the criteria in Table 1. The ‘h’ refers to the location where sheet height would be measured for this surface parallel fracture. B. Example of fractures that may appear to be a single fracture (left), but upon close examination are in fact multiple fractures intersecting and/or separated by rock (right inset). Arrow points to the location of the inset image on the main image. Compass in the foreground for scale.

Fig. 3. Example histograms and statistics of fracture length data measured on the exposed surfaces of clasts 15-50 cm max diameter. Upper row are data for clasts found on a modern ephemeral stream boulder bar. Clasts overall have very low fracture number density. Lower row are data for clasts on an ~6 ka surface where fracture number density is much higher. Note that it takes about 100 clasts to arrive at a statistically significant power law distribution for the Modern Wash clasts, but only 5 rocks for the rocks with higher fracture densities. Producing histograms interactively as data is collected can help establish how many observation areas are necessary for a given site.

Fig. 4. Reduced size image of an 8.5” x 11” ‘fracture sheet’ to be employed in the field to increase efficiency and to reduce ‘missing’ data. Sheet templates for both clasts and outcrops that can be modified are provided in Data Supplement as well as a data-entry template.

Fig. 5. Visual aid for estimating the abundance of “countable” rock features – including fractures. An index of 0-4 is assigned depending on the abundance of features within an average of any given observation area (ex: 10 x 10 cm) on the clast or window being examined. The area of observation is defined by the size of the features being measured. A 10 cm x 10 cm square is used for estimating the abundance of ‘fractures < 2 cm’ defined as fractures with lengths of >0.5 cm but < 2 cm (see section 5.2 for details of how to use the index). For features  $\leq 0.5$  cm, a 1 cm x 1 cm area would be employed and for features  $\geq 2$  cm, a 1 x 1 m area.

Fig. 6. A visual percent estimator (modified from Terry and Chilingar, 1955). Estimator should be employed in every estimate of percentages. See section 5.2 for using the estimator to assign a percent coverage index to features that are not countable or vary in size (e.g., lichen coverage, fine mafic minerals, etc.).

Fig. 7. **Inset:** Roundness and sphericity chart – modified from Krumbein and Sloss (1951) to add the roundness and sphericity lettering. **Roundness:** A = angular; SA = subangular; SR = subrounded; R = rounded; WR = well-rounded. **Sphericity:** S = spherical; SS = subspherical; SE = sub-elongate; E = elongate. **Edges:** fracture comparator whereby the width most closely matching the fracture aperture is noted. Note: a to-scale pdf is available in the Data Supplement, however, owing to printing and publication scaling, it is highly recommended to calibrate the comparator prior to using it in the field.

Fig. 8 Depiction of types of fracture intersection nodes. I-nodes comprise fracture terminations with no connections. Y-nodes are abutting fractures that do not cross. X-nodes are fractures that cross. C-nodes are ‘contingent nodes’ defined by the user. In this example the rule is related to the distance between I-nodes. For #1, the distance is wider than the criteria, so the terminations are designated as I-nodes. For #2, the distance is within the limits, and the ‘connection’ is designated as a C-node.

Fig. 9. Examples of aperture transects that are appropriate for measurement of fracture aperture widths (green) and transects where there is evidence that the fracture walls have been eroded or chipped and therefore should not be employed for a width

1156 measurement (red). In cases where it is not clear if erosion or chipping has occurred (orange), a note can be made for the fracture  
1157 width to possibly eliminate outliers during data analysis.

1158

1159

1160 Fig. 10. Box and whisker plots of case example data collected by five different pairs of workers on the same geomorphic surface.

1161 "x"s mark the means. Groups 1-4 were novice workers. Group 5 comprised one experienced worker. A. Fracture lengths B.

1162 Fractures per rock C. Clast length

1163

1164

1165 *Table 1. List of proposed rule-based criteria for defining measurable fractures*

<b>The answer to the following questions must be ‘yes’ for all measured fractures. Measure all fractures meeting these criteria within the observation area.</b>	<b><u>NOTES</u></b>
<ul style="list-style-type: none"> <li>• Is the feature a lineament longer than it is wide?</li> <li>• Does the lineament contain open space bounded by walls?</li> <li>• If the lineament is not open, can the infilling material (ex: dust and lichens) be readily scraped out?</li> <li>• If the lineament is open or after the material has been scraped out, is the opening deeper than it is wide <u>and</u> bounded by ~parallel walls?</li> <li>• Is the open portion of the lineament <math>\geq 2</math> cm (<math>&gt;10</math> grains) in length (without interrupting bridges of rock or cemented infilling material)?</li> </ul>	Do not measure: <ul style="list-style-type: none"> <li>• Spherical pores/vesicles.</li> <li>• Lineaments, or portions of lineaments, with solid mineral infilling/cement.</li> <li>• Ledge edges or linear etchings.</li> <li>• rock bridges between fractures</li> </ul>

1166

1167 *Table 2. List of proposed data to collect for the rock observation area and for all fractures  $\geq 2$  cm in length*

<b>Rock Observations</b>	<b>Individual Fracture Observations</b>
<ul style="list-style-type: none"> <li>• Dimensions of the observation area (e.g. clast, outcrop, and/or window length, width, height)</li> <li>• Rock type</li> <li>• Grain size</li> <li>• Mineralogy % (minimally felsic vs. mafic)</li> <li>• Sphericity of exposure</li> <li>• Roundness of exposure</li> <li>• Fabric description, strike, and dip (e.g. vein, foliation, bedding)</li> <li>• Granular Disintegration</li> <li>• Pitting</li> <li>• Lichen and Varnish</li> <li>• Fracture Connectivity</li> <li>• Fracture Spacing</li> </ul>	<ul style="list-style-type: none"> <li>• Length (surface exposure length measured with a flexible tape)</li> <li>• Aperture width: center and maximum widths measured with calipers and/or comparator</li> <li>• Strike 0-360° (right-hand rule preferred)</li> <li>• Dip 0-90°</li> <li>• Parallelism (note features parallel to the fracture such as fabric, rock faces)</li> <li>• Sheet height (the thickness of what would be the detached spall or sheet of rock above a surface parallel fracture)</li> <li>• Weathering Index</li> </ul>

1168

1169

1170

1171

*Table 3. List of field equipment*

<b>Required</b>	<b>Recommended</b>
<ul style="list-style-type: none"> <li>• Hand lens (large, 10x)</li> <li>• Grain size card</li> <li>• Fracture comparator (for fracture widths)</li> <li>• Flexible seamstress tape measure (with mm)</li> <li>• Calipers (mm 0.0 to 150)</li> <li>• Brunton or similar compass</li> <li>• Roundness and sphericity chart</li> <li>• Visual percentage estimator</li> <li>• Fracture sheets</li> </ul>	<ul style="list-style-type: none"> <li>• Camera with macro lens</li> <li>• Chalk for marking measured fractures and windows</li> <li>• Safety pin or needle for fracture exploration</li> <li>• Cardboard cutout frames for windows</li> <li>• Small white board or chalk board for including observation area ID in photos</li> </ul>

1172

1173

**1174 Bibliography**

- 1175** Aich, S. and Gross, M. R.: Geospatial analysis of the association between bedrock fractures and vegetation in an arid environment, **1176** *International Journal of Remote Sensing*, 29, 6937-6955, 10.1080/01431160802220185, 2008.
- 1177** Al-Fahmi, M. M., Hooker, J. N., Al-Mojel, A. S., and Cartwright, J. A.: New scaling of fractures in a giant carbonate platform **1178** from outcrops and subsurface, *Journal of Structural Geology*, 140, 104142, <https://doi.org/10.1016/j.jsg.2020.104142>, 2020.
- 1179** Aldred, J., Eppes, M. C., Aquino, K., Deal, R., Garbini, J., Swami, S., Tuttle, A., and Xanthos, G.: The influence of solar-induced **1180** thermal stresses on the mechanical weathering of rocks in humid mid-latitudes, *Earth Surface Processes and Landforms*, 41, 603- **1181** 614, 2015.
- 1182** Alneasani, M. and Behnia, M.: An experimental investigation on tensile fracturing of brittle rocks by considering the effect of grain **1183** size and mineralogical composition, *International Journal of Rock Mechanics and Mining Sciences*, 137, 104570, **1184** <https://doi.org/10.1016/j.ijrmms.2020.104570>, 2021.
- 1185** Anderson, T. L.: *Fracture Mechanics: Fundamentals and Applications*, Third, Taylor & Francis Group, Boca Raton, FL, 2005.
- 1186** Anders, M. H., Laubach, S. E., and Scholz, C. H., : Microfractures: a review. *Journal of Structural Geology*, 69, Part B, 377-394. **1187** doi: 10.1016/j.jsg.2014.05.011, 2014.
- 1188** Andresen, C. A., Hansen, A., Le Goc, R., Davy, P., and Hope, S. M.: Topology of fracture networks, *Frontiers in physics*, 1, 7, **1189** 10.3389/fphy.2013.00007, 2013.
- 1190** Andrews, B. J., Roberts, J. J., Shipton, Z. K., Bigi, S., Tartarello, M. C., and Johnson, G.: How do we see fractures? Quantifying **1191** subjective bias in fracture data collection, *Solid Earth*, 10, 487, 2019.
- 1192** ASTM: D7012-14: Standard Test Methods for Compressive Strength and Elastic Moduli of Intact Rock Core Specimens Under **1193** Varying States of Stress and Temperatures, 2017.
- 1194** Atkinson, B. K.: *Fracture Mechanics of Rock*, Academic Press Geology Series, Academic Press Inc., Orlando, Florida, **1195** <https://doi.org/10.1016/C2009-0-21691-6>, 1987.
- 1196** Ayatollahi, M. R. and Akbardoost, J.: Size and geometry effects on rock fracture toughness: Mode I fracture, *Rock Mechanics and **1197*** *Rock Engineering*, 47, 677-687, 10.1007/s00603-013-0430-7, 2014.
- 1198** Aydin, A. and Basu, A.: The Schmidt hammer in rock material characterization, *Engineering Geology*, 81, 1-14, **1199** <https://doi.org/10.1016/j.enggeo.2005.06.006>, 2005.
- 1200** Baecher, G. B.: Statistical analysis of rock mass fracturing, *Journal of the International Association for Mathematical Geology*, 15, **1201** 329-348, 10.1007/BF01036074, 1983.
- 1202** Balco, G.: Technical note: A prototype transparent-middle-layer data management and analysis infrastructure for cosmogenic- **1203** nuclide exposure dating, *Geochronology*, 2, 169-175, <https://doi.org/10.5194/gchron-2-169-2020>, 2020.
- 1204** Barthélémy, J.-F., Guiton, M. L. E., and Daniel, J.-M.: Estimates of fracture density and uncertainties from well data, *International **1205*** *Journal of Rock Mechanics and Mining Sciences*, 46, 590-603, <https://doi.org/10.1016/j.ijrmms.2008.08.003>, 2009.
- 1206** Barton, C. C. and Hsieh, P. A.: *Physical and Hydrologic-Flow Properties of Fractures: Las Vegas, Nevada - Zion Canyon, Utah - **1207*** *Grand Canyon, Arizona - Yucca Mountain, Nevada, July 20-24, 1989 (Field Trip Guidebook T385)*, American Geophysical Union, **1208** Washington, D.C.1989.
- 1209** Barton, C. C., Larsen, E., Page, W. R., and Howard, T. M.: Characterizing fractured rock for fluid-flow, geomechanical, and **1210** paleostress modeling: Methods and preliminary results from Yucca Mountain, Nevada, United States, Medium: ED; Size: 74 p., **1211** 10.2172/145208, 1993.
- 1212** Bell, F.G.: *Engineering Geology*, 2nd edition. Butterworth-Heinemann Press, Burlington, MA, USA. 581 p. ISBN 978-0-7506- **1213** 8077-6. 2007.
- 1214** Berberich, S.: A chronosequence of cracking in Mill Creek, California, *Geography and Earth Sciences*, The University of North **1215** Carolina Charlotte, ProQuest, 2020.
- 1216** Berkowitz, B.: Characterizing flow and transport in fractured geological media: A review, *Advances in Water Resources*, 25, 861- **1217** 884, [https://doi.org/10.1016/S0309-1708\(02\)00042-8](https://doi.org/10.1016/S0309-1708(02)00042-8), 2002.

- 1218** Betlem, P., Birchall, T., Lord, G., Oldfield, S., Nakken, L., Ogata, K., and Senger, K.: High resolution digital outcrop model of faults and fractures in caprock shales, Konusdalen West, central Spitsbergen, Earth Syst. Sci. Data Discuss. [preprint], **1219** <https://doi.org/10.5194/essd-2022-143>, in review, 2022.
- 1220**
- 1221** Birkeland, P. W.: Soils and Geomorphology, Oxford University Press, New York, New York, 1999.
- 1222** Bonnet, E., Bour, O., Odling, N. E., Davy, P., Main, I., Cowie, P., and Berkowitz, B.: Scaling of fracture systems in geological **1223** media, Reviews of Geophysics, 39, 347-383, 2001.
- 1224** Borg, I. and Handin, J.: Experimental deformation of crystalline rocks, Tectonophysics, 3, 249-367, [https://doi.org/10.1016/0040-1951\(66\)90019-9](https://doi.org/10.1016/0040-1951(66)90019-9), 1966. **1225**
- 1226** Brantley, S. L., Eissenstat, D. M., Marshall, J. A., Godsey, S. E., Balogh-Brunstad, Z., Karwan, D. L., Papuga, S. A., Roering, J., **1227** Dawson, T. E., Evaristo, J., Chadwick, O., McDonnell, J. J., and Weathers, K. C.: Reviews and syntheses: On the roles trees play **1228** in building and plumbing the critical zone, Biogeosciences, 14, 5115, 2017.
- 1229** Brantut, N., P. Baud, M. J. Heap, and Meredith, P. G.: Micromechanics of brittle creep in rocks, J. Geophys. Res. 117, B08412, **1230** doi:10.1029/2012JB009299, 2012.
- 1231** Brantut, N., Heap, M. J., Meredith, P. G., and Baud, P.: Time-dependent cracking and brittle creep in crustal rocks: A review, **1232** Journal of Structural Geology, 52, 17-43, 2013.
- 1233** Brilha, J., Gray, M., Pereira, D. I., and Pereira, P.: Geodiversity: An integrative review as a contribution to the sustainable **1234** management of the whole of nature, Environmental Science & Policy, 86, 19-28, <https://doi.org/10.1016/j.envsci.2018.05.001>, **1235** 2018.
- 1236** Buckman, S., Morris, R. H., and Bourman, R. P.: Fire-induced rock spalling as a mechanism of weathering responsible for flared **1237** slope and inselberg development, Nature Communications, 12, 2150, 10.1038/s41467-021-22451-2, 2021.
- 1238** Burghelea, C., Zaharescu, D. G., Dontsova, K., Maier, R., Huxman, T., and Chorover, J.: Mineral nutrient mobilization by plants **1239** from rock: influence of rock type and arbuscular mycorrhiza, Biogeochemistry, 124, 187-203, 10.1007/s10533-015-0092-5, 2015.
- 1240** Burke, R. M. and Birkeland, P. W.: Reevaluation of multiparameter relative dating techniques and their application to the glacial **1241** sequence along the eastern escarpment of the Sierra Nevada, California, Quaternary Research, 11, 21-51, 10.1016/0033-5894(79)90068-1, 1979. **1242**
- 1243** Burnett, B. N., Meyer, G. A., and McFadden, L. D.: Aspect-related microclimatic influences on slope forms and processes, **1244** northeastern Arizona, Journal of Geophysical Research: Earth Surface, 113, <https://doi.org/10.1029/2007JF000789>, 2008.
- 1245** Buss, H. L., Sak, P. B., Webb, S. M., and Brantley, S. L.: Weathering of the Rio Blanco quartz diorite, Luquillo Mountains, Puerto **1246** Rico: Coupling oxidation, dissolution, and fracturing, Geochimica et Cosmochimica Acta, 72, 4488-4507, 2008.
- 1247** Chen, X., Eichhubl, P., and Olson, J. E.: Effect of water on critical and subcritical fracture properties of Woodford shale, Journal **1248** of Geophysical Research: Solid Earth, 122, 2736-2750, <https://doi.org/10.1002/2016JB013708>, 2017.
- 1249** Chilton, K. D. and Spotila, J. A.: Preservation of Valley and Ridge topography via delivery of resistant, ridge-sourced boulders to **1250** hillslopes and channels, Southern Appalachian Mountains, U.S.A, Geomorphology, 365, 107263, **1251** <https://doi.org/10.1016/j.geomorph.2020.107263>, 2020.
- 1252** Clauset, A., Shalizi, C. R., and Newman, M. E. J.: Power-law distributions in empirical data, SIAM review, 51, 661-703, **1253** 10.1137/070710111, 2009.
- 1254** Collins, B. D. and Stock, G. M.: Rockfall triggering by cyclic thermal stressing of exfoliation fractures, Nature Geoscience, 9, 395- **1255** 401, 2016.
- 1256** Coombes, M. A., Viles, H. A., and Zhang, H.: Thermal blanketing by ivy (*Hedera helix* L.) can protect building stone from **1257** damaging frosts, Nature: Scientific Reports, 8, 1-12, 2018.
- 1258** Corrêa, R. S. M., Marrett, R., and Laubach, S. E.: Analysis of spatial arrangement of fractures in two dimensions using point **1259** process statistics, Journal of Structural Geology, 163, 104726, <https://doi.org/10.1016/j.jsg.2022.104726>, 2022.
- 1260** Cox, R., Lopes, W. A., and Jahn, K. L.: Quantitative roundness analysis of coastal boulder deposits, Marine Geology, 396, 114- **1261** 141, <https://doi.org/10.1016/j.margeo.2017.03.003>, 2018.
- 1262** Cuccuru, S., Casini, L., Oggiano, G., and Cherchi, G. P.: Can weathering improve the toughness of a fractured rock? A case study **1263** using the San Giacomo granite, Bulletin of Engineering Geology Environments, 71, 557-567, 2012.

- 1264** Davy, P., Le Goc, R., Darcel, C., Bour, O., de Dreuzy, J. R., and Munier, R.: A likely universal model of fracture scaling and its  
**1265** consequence for crustal hydromechanics, *Journal of Geophysical Research: Solid Earth*, 115,  
**1266** <https://doi.org/10.1029/2009JB007043>, 2010.
- 1267** Deere, D.U.: Technical description of cores for engineering purposes. *Rock Mechanics and Engineering Geology*, 1, 18-22, 1964.
- 1268** Dershowitz, W. S. and Herda, H. H.: Interpretation of fracture spacing and intensity, *The 33rd U.S. Symposium on Rock Mechanics*  
**1269** (USRMS), 1992.
- 1270** DiBiase, R. A., Rossi, M. W., and Neely, A. B.: Fracture density and grain size controls on the relief structure of bedrock  
**1271** landscapes, *Geology*, 48, 399-402, 2018.
- 1272** Domokos, G., Jerolmack, D. J., Kun, F., and Torok, J.: Plato's cube and the natural geometry of fragmentation, *Proceedings of the*  
**1273** *National Academy of Sciences*, 117, 18178-18185, 2020.
- 1274** Dove, P. M.: Geochemical controls on the kinetics of quartz fracture at subcritical tensile stresses, *Journal of Geophysical Research*,  
**1275** 100, 349-359, 1995.
- 1276** Engelder, T.: *Stress Regimes in the Lithosphere*, Princeton University Press, 1993.
- 1277** Engelder, T.: Tectonic implications drawn from differences in the surface morphology on two joint sets in the Appalachian Valley  
**1278** and Ridge, Virginia, *Geology*, 32(5), 413-416, 2004.
- 1279** English, J. M. and Laubach, S. E.: Opening-mode fracture systems: insights from recent fluid inclusion microthermometry studies  
**1280** of crack-seal fracture cements, *Geological Society, London, Special Publications*, 458, 257-272, doi:10.1144/SP458.1, 2017.
- 1281** Eppes, M.-C., 2022. Mechanical Weathering: A Conceptual Overview. In: Shroder, J.J.F. (Ed.), *Treatise on Geomorphology*, vol.  
**1282** 3. Elsevier, Academic Press, pp. 30–45. <https://dx.doi.org/10.1016/B978-0-12-818234-5.00200-5>.
- 1283** Eppes, M. C. and Griffing, D.: Granular disintegration of marble in nature: A thermal-mechanical origin for a grus and corestone  
**1284** landscape, *Geomorphology*, 117, 170-180, 2010.
- 1285** Eppes, M. C. and Keanini, R.: Mechanical weathering and rock erosion by climate-dependent subcritical cracking, *Reviews of*  
**1286** *Geophysics*, 55, 470-508, 2017.
- 1287** Eppes, M. C., McFadden, L. D., Wegmann, K. W., and Scuderi, L. A.: Cracks in desert pavement rocks: Further insights into  
**1288** mechanical weathering by directional insolation, *Geomorphology*, 123, 97-108, 2010.
- 1289** Eppes, M. C., Magi, B., Scheff, J., Warren, K., Ching, S., and Feng, T.: Warmer, wetter climates accelerate mechanical weathering  
**1290** in field data, independent of stress-loading, *Geophysical Research Letters*, 47, 1-11, 2020.
- 1291** Eppes, M. C., Magi, B., Hallet, B., Delmelle, E., Mackenzie-Helnwein, P., Warren, K., and Swami, S.: Deciphering the role of  
**1292** solar-induced thermal stresses in rock weathering, *GSA Bulletin*, 128, 1315-1338, 2016.
- 1293** Eppes, M. C., Hancock, G. S., Chen, X., Arey, J., Dewers, T., Huettenmoser, J., Kiessling, S., Moser, F., Tannu, N., Weiserbs, B.,  
**1294** and Whitten, J.: Rates of subcritical cracking and long-term rock erosion, *Geology*, 46, 951-954, 2018.
- 1295** Fisher, N. I.: *Statistical Analysis of Circular Data*, Cambridge University Press, Cambridge, England,  
**1296** <https://doi.org/10.1017/CBO9780511564345>, 1993.
- 1297** Forstner, S. R. and Laubach, S. E.: Scale-dependent fracture networks, *Journal of Structural Geology*, 165, 104748,  
**1298** <https://doi.org/10.1016/j.jsg.2022.104748>, 2022.
- 1299** Girard, L., Gruber, S., Weber, S., and Beutel, J.: Environmental controls of frost cracking revealed through in situ acoustic emission  
**1300** measurements in steep bedrock, *Geophysical Research Letters*, 40, 1748-1753, 10.1002/grl.50384, 2013.
- 1301** Gischig, V. S., Moore, J. R., Evans, K. F., Amann, F., and Loew, S.: Thermomechanical forcing of deep rock slope deformation:  
**1302** 1. Conceptual study of a simplified slope, *Journal of Geophysical Research*, 116, 10.1029/2011JF002006, 2011.
- 1303** Glade, R. C., Shobe, C. M., Anderson, R. S., and Tucker, G. E.: Canyon shape and erosion dynamics governed by channel-hillslope  
**1304** feedbacks, *Geology*, 47, 650-654, 10.1130/G46219.1, 2019.
- 1305** Gomez, L. A., and Laubach, S. E.: Rapid digital quantification of microfracture populations, *Journal of Structural Geology*, 28,  
**1306** 408-420, 2006.
- 1307** Gomez-Heras, M., Smith, B. J., and Fort, R.: Surface temperature differences between minerals in crystalline rocks: Implications  
**1308** for granular disaggregation of granites through thermal fatigue, *Geomorphology*, 78, 236-249, 2006.

- 1309** Gómez-Pujol, L., Fornós, J. J., and Swantesson, J. O. H.: Rock surface millimetre-scale roughness and weathering of supratidal  
**1310** Mallorcan carbonate coasts (Balearic Islands), *Earth Surface Processes and Landforms*, 31, 1792-1801,  
**1311** <https://doi.org/10.1002/esp.1379>, 2006.
- 1312** Griffiths, L., Heap, M. J., Baud, P., and Schmittbuhl, J.: Quantification of microcrack characteristics and implications for stiffness  
**1313** and strength of granite, *International Journal of Rock Mechanics and Mining Sciences*, 100, 138-150,  
**1314** <https://doi.org/10.1016/j.ijrmms.2017.10.013>, 2017.
- 1315** Hancock, G. S. and Kirwan, M.: Summit erosion rates deduced from <sup>10</sup>Be: Implications for relief production in the central  
**1316** Appalachians, *Geology*, 35, 89-92, 10.1130/g23147a.1, 2007.
- 1317** Hancock, P. L.: Brittle microtectonics: Principles and practice, *Journal of Structural Geology*, 7, 437-457,  
**1318** [https://doi.org/10.1016/0191-8141\(85\)90048-3](https://doi.org/10.1016/0191-8141(85)90048-3), 1985.
- 1319** Handin, J. and Hager, R. V., Jr.: Experimental deformation of sedimentary rocks under confining pressure: Tests at room  
**1320** temperature on dry samples, *AAPG Bulletin*, 41, 1-50, 10.1306/5ceae5fb-16bb-11d7-8645000102c1865d, 1957.
- 1321** Handin, J. and Hager, R. V., Jr.: Experimental deformation of sedimentary rocks under confining pressure: Tests at high  
**1322** temperature, *AAPG Bulletin*, 42, 2892-2934, 10.1306/0bda5c27-16bd-11d7-8645000102c1865d, 1958.
- 1323** Handin, J., Hager Jr, R. V., Friedman, M., and Feather, J. N.: Experimental deformation of sedimentary rocks under confining  
**1324** pressure: Pore pressure tests, *AAPG Bulletin*, 47, 717-755, 1963.
- 1325** Hasenmueller, E. A., Gu, X., Weitzman, J. N., Adams, T. S., Stinchcomb, G. E., Eissenstat, D. M., Drohan, P. J., Brantley, S. L.,  
**1326** and Kaye, J. P.: Weathering of rock to regolith: The activity of deep roots in bedrock fractures, *Geoderma*, 300, 11-31,  
**1327** <https://doi.org/10.1016/j.geoderma.2017.03.020>, 2017.
- 1328** Hatir, M. E.: Determining the weathering classification of stone cultural heritage via the analytic hierarchy process and fuzzy  
**1329** inference system, *Journal of Cultural Heritage*, 44, 120-134, <https://doi.org/10.1016/j.culher.2020.02.011>, 2020.
- 1330** He, M., Xia, H., Jia, X., Gong, W., Zhao, F., and Liang, K.: Studies on classification, criteria, and control of rockbursts, *Journal of*  
**1331** *Rock Mechanics and Geotechnical Engineering*, 4, 97-114, 10.3724/SP.J.1235.2012.00097, 2012.
- 1332** Healy, D., Rizzo, R. E., Cornwell, D. G., Farrell, N. J. C., Watkins, H., Timms, N. E., Gomez-Rivas, E., and Smith, M.: FracPaQ:  
**1333** A MATLAB™ toolbox for the quantification of fracture patterns, *Journal of Structural Geology*, 95, 1-16,  
**1334** <https://doi.org/10.1016/j.jsg.2016.12.003>, 2017.
- 1335** Heard, H. C.: Effect of large changes in strain rate in the experimental deformation of Yule Marble, *The Journal of Geology*, 71,  
**1336** 162-195, 1963.
- 1337** Hencher, S.: *Practical Engineering Geology*. Spon Press, New York, NY, USA. 450 p. ISBN 97800-203-89482-8. 2015.
- 1338** Hencher, S.: *Practical Rock Mechanics*. Spon Press, New York, NY, USA. 356 p. ISBN 978-1-4822-1726-1. 2019.
- 1339** Heidbach, O., Rajabi, M., Cui, X., Fuchs, K., Müller, B., Reinecker, J., Reiter, K., Tingay, M., Wenzel, F., Xie, F., Ziegler, M. O.,  
**1340** Zoback, M.-L., and Zoback, M.: The World Stress Map database release 2016: Crustal stress pattern across scales, *Tectonophysics*,  
**1341** 744, 484-498, <https://doi.org/10.1016/j.tecto.2018.07.007>, 2018.
- 1342** Holder, J., Olson, J. E., and Philip, Z.: Experimental determination of subcritical crack growth parameters in sedimentary rock,  
**1343** *Geophysical Research Letters*, 28, 599-602, <https://doi.org/10.1029/2000GL011918>, 2001.
- 1344** Hooke, R.: Geomorphic evidence for Late-Wisconsin and Holocene tectonic deformation, Death Valley, California, *GSA Bulletin*,  
**1345** 83, 2073-2098, 10.1130/0016-7606(1972)83[2073:Geflah]2.0.Co;2, 1972.
- 1346** Hooker, J. N., Laubach, S. E., and Marrett, R.: A universal power-law scaling exponent for fracture apertures in sandstones, *GSA*  
**1347** *Bulletin*, 126, 1340-1362, 10.1130/b30945.1, 2014.
- 1348** Hooker, J. N., Gale, J. F. W., Gomez, L. A., Laubach, S. E., Marrett, R., and Reed, R. M.: Aperture-size scaling variations in a  
**1349** low-strain opening-mode fracture set, Cozzette Sandstone, Colorado, *Journal of Structural Geology*, 31, 707-718,  
**1350** <https://doi.org/10.1016/j.jsg.2009.04.001>, 2009.
- 1351** Hooker, J.N., Laubach, S.E., and Marrett, R.: Fracture-aperture size–frequency, spatial distribution, and growth processes in strata-  
**1352** bounded and non-strata-bounded fractures, Cambrian Mesón Group, NW Argentina, *Journal of Structural Geology*, 54, 54-71.  
**1353** [doi.org/10.1016/j.jsg.2013.06.011](https://doi.org/10.1016/j.jsg.2013.06.011), 2013.
- 1354** Isherwood, D. and Street, A.: Biotite-induced grossification of the Boulder Creek Granodiorite, Boulder County, Colorado, *GSA*  
**1355** *Bulletin*, 87, 366-370, 10.1130/0016-7606(1976)87<366:Bgotbc>2.0.Co;2, 1976.

- 1356** Janio de Castro Lima, J. and Paraguassú, A. B.: Linear thermal expansion of granitic rocks: influence of apparent porosity, grain size and quartz content, *Bulletin of Engineering Geology and the Environment*, 63, 215-220, [10.1007/s10064-004-0233-x](https://doi.org/10.1007/s10064-004-0233-x), 2004.
- 1357**
- 1358** Jenny, H.: *Factors of Soil Formation: A System of Quantitative Pedology*, McGraw-Hill, New York, New York, 1941.
- 1359** Kobayashi, A. S. and Enetanya, A. N.: Stress intensity factor of a corner crack, *Mechanics of Crack Growth*, 1976.
- 1360** Kranz, R. L.: Microcrack in rocks: A review, *Tectonophysics*, 100, 449-480, 1983.
- 1361** Krumbein, W. C.: Fundamental attributes of sedimentary particles, *University of Iowa Student Engineering Bulletin*, 27, 318-331, 1943.
- 1362**
- 1363** Krumbein, W. C. and Sloss, L. L.: *Stratigraphy and Sedimentation*, W. H. Freeman and Company, San Francisco, California, 1951.
- 1364** Lamp, J. L., Marchant, D. R., Mackay, S. L., and Head, J. W.: Thermal stress weathering and the spalling of Antarctic rocks, *Journal of Geophysical Research: Earth Surface*, 122, 3-24, <https://doi.org/10.1002/2016JF003992>, 2017.
- 1365**
- 1366** Laubach, S. E., Olson, J. E., and Gross, M. R.: Mechanical and fracture stratigraphy, *AAPG Bulletin*, 93, 1413-1426, [10.1306/07270909094](https://doi.org/10.1306/07270909094), 2009.
- 1367**
- 1368** Laubach, S. E., Lamarche, J., Gauthier, B. D. M., Dunne, W. M., and Sanderson, D. J.: Spatial arrangement of faults and opening-mode fractures, *Journal of Structural Geology*, 108, 2-15, <https://doi.org/10.1016/j.jsg.2017.08.008>, 2018.
- 1369**
- 1370** Laubach, S. E., Lander, R. H., Criscenti, L. J., Anovitz, L. M., Urai, J. L., Pollyea, R. M., Hooker, J. N., Narr, W., Evans, M. A., Kerisit, S. N., Olson, J. E., Dewers, T., Fisher, D., Bodnar, R., Evans, B., Dove, P., Bonnell, L. M., Marder, M. P., and Pyrak-Nolte, L.: The role of chemistry in fracture pattern development and opportunities to advance interpretations of geological materials, *Reviews of Geophysics*, 57, 1065-1111, [10.1029/2019RG000671](https://doi.org/10.1029/2019RG000671), 2019.
- 1371**
- 1372**
- 1373**
- 1374** Leith, K., Moore, J. R., Amann, F., and Loew, S.: In situ stress control on microcrack generation and macroscopic extensional fracture in exhuming bedrock, *Journal of Geophysical Research*, 119, 1-22, 2014.
- 1375**
- 1376** Leone, J. D., Holbrook, W. S., Reibe, C. S., Chorover, J., Ferre, T. P. A., Carr, B. J., and Callahan, R. P.: Strong slope-aspect control of regolith thickness by bedrock foliation, *Earth Surface Processes and Landforms*, 45, 2998-3010, 2020.
- 1377**
- 1378** Long, J., Jones, R., Daniels, S., Gilment, S., Oxlade, D., and Wilkinson, M.: Reducing uncertainty in fracture modelling: Assessing user bias in interpretations from satellite imagery, *AAPG 2019 Annual Convention & Exhibition*, San Antonio, TX, 2019.
- 1379**
- 1380** Long, J. C. S. and Witherspoon, P. A.: The relationship of the degree of interconnection to permeability in fracture networks, *Journal of Geophysical Research: Solid Earth*, 90, 3087-3098, <https://doi.org/10.1029/JB090iB04p03087>, 1985.
- 1381**
- 1382** Macholdt, D. S., Al-Amri, A. M., Tuffaha, H. T., Jochum, K. P., and Andreae, M. O.: Growth of desert varnish on petroglyphs from Jubbah and Shuwaymis, Ha'il region, Saudi Arabia, *The Holocene*, 28, 1495-1511, [10.1177/0959683618777075](https://doi.org/10.1177/0959683618777075), 2018.
- 1383**
- 1384** Maffucci, R., Bigi, S., Corrado, S., Chiodi, A., Di Paolo, L., Giordano, G., and Invernizzi, C.: Quality assessment of reservoirs by means of outcrop data and "discrete fracture network" models: The case history of Rosario de La Frontera (NW Argentina) geothermal system, *Tectonophysics*, 647-648, 112-131, <https://doi.org/10.1016/j.tecto.2015.02.016>, 2015.
- 1385**
- 1386**
- 1387** Manzocchi, T.: The connectivity of two-dimensional networks of spatially correlated fractures, *Water Resources Research*, 38, 1-1-1-20, <https://doi.org/10.1029/2000WR000180>, 2002.
- 1388**
- 1389** Mardia, K. V. and Jupp, P. E.: *Directional Statistics*, Academic Press Inc., London, England, 1972.
- 1390** Marrett, R., Gale, J. F. W., Gómez, L. A., and Laubach, S. E.: Correlation analysis of fracture arrangement in space, *Journal of Structural Geology*, 108, 16-33, <https://doi.org/10.1016/j.jsg.2017.06.012>, 2018.
- 1391**
- 1392** Marshall, J., Clyne, J., Eppes, M. C., and Dawson, T.: Barking up the wrong tree? Tree root tapping, subcritical cracking, and potential influence on bedrock porosity, *AGU 2021 Fall Abstracts*, 2021a.
- 1393**
- 1394** Marshall, J. A., Roering, J. J., Rempel, A. W., Shafer, S. L., and Bartlein, P. J.: Extensive frost weathering across unglaciated North America during the Last Glacial Maximum, *Geophysical Research Letters*, 48, <https://doi.org/10.1029/2020GL090305>, 2021b.
- 1395**
- 1396**
- 1397** Martel, S. J.: Effect of topographic curvature on near-surface stresses and application to sheeting joints, *Geophysical Research Letters*, 33, 2006.
- 1398**
- 1399** Martel, S. J.: Mechanics of curved surfaces, with application to surface-parallel cracks, *Geophysical Research Letters*, 38, 2011.
- 1400** Martel, S. J.: Progress in understanding sheeting joints over the past two centuries, *Journal of Structural Geology*, 94, 68-86, 2017.



- 1401** Matsuoka, N. and Murton, J.: Frost weathering: Recent advances and future directions, *Permafrost and Periglacial Processes*, 19, 195-210, 10.1002/ppp.620, 2008.
- 1402**
- 1403** Matthews, J. A. and Winkler, S.: Schmidt-hammer exposure-age dating: A review of principles and practice, *Earth-Science Reviews*, 230, 104038, <https://doi.org/10.1016/j.earscirev.2022.104038>, 2022.
- 1404**
- 1405** McAuliffe, J. R., McFadden, L. D., Persico, L. P., and Rittenour, T. M.: Climate and vegetation change, hillslope soil erosion, and the complex nature of Late Quaternary environmental transitions, Eastern Mojave Desert, USA, *Quaternary*, 5, 43, 2022.
- 1406**
- 1407** McCarroll, D.: The Schmidt hammer, weathering, and rock surface roughness, *Earth Surface Processes and Landforms*, 16, 477-480, <https://doi.org/10.1002/esp.3290160510>, 1991.
- 1408**
- 1409** McFadden, L. D. and Hendricks, D. M.: Changes in the content and composition of pedogenic iron oxyhydroxides in a chronosequence of soils in southern California, *Quaternary Research*, 23, 189-204, [https://doi.org/10.1016/0033-5894\(85\)90028-6](https://doi.org/10.1016/0033-5894(85)90028-6), 1985.
- 1410**
- 1411**
- 1412** McFadden, L. D., Eppes, M. C., Gillespie, A. R., and Hallet, B.: Physical weathering in arid landscapes due to diurnal variation in the direction of solar heating, *GSA Bulletin*, 117, 161-173, 2005.
- 1413**
- 1414** Mogi, K.: Effect of the intermediate principal stress on rock failure, *Journal of Geophysical Research (1896-1977)*, 72, 5117-5131, <https://doi.org/10.1029/JZ072i020p05117>, 1967.
- 1415**
- 1416** Mogi, K.: Fracture and flow of rocks under high triaxial compression, *Journal of Geophysical Research (1896-1977)*, 76, 1255-1269, <https://doi.org/10.1029/JB076i005p01255>, 1971.
- 1417**
- 1418** Molaro, J. L., Byrne, S., and Le, J.-L.: Thermally induced stresses in boulders on airless body surfaces, and implications for rock breakdown, *Icarus*, 294, 247-261, 2017.
- 1419**
- 1420** Molaro, J. L., Hergenrother, C. W., Chesley, S. R., Walsh, K. J., Hanna, R. D., Haberle, C. W., Schwartz, S. R., Ballouz, R.-L., Bottke, W. F., Campins, H. J., and Lauretta, D. S.: Thermal fatigue as a driving mechanism for activity on asteroid Bennu, *Journal of Geophysical Research*, 125, 1-24, 10.1029/2019JE006325, 2020.
- 1421**
- 1422**
- 1423** Molnar, P.: Interactions among topographically induced elastic stress, static fatigue, and valley incision, *Journal of Geophysical Research*, 109, 1-9, 10.1029/2003JF000097, 2004.
- 1424**
- 1425** Moon, S., Perron, J. T., Martel, S. J., Goodfellow, B. W., Ivars, D. M., Hall, A., Heyman, J., Munier, R., Naslund, J., Simeonov, A., and Stroeven, A. P.: Present-day stress field influences bedrock fracture openness deep into the subsurface, *Geophysical Research Letters*, 47, 1-10, 2020.
- 1426**
- 1427**
- 1428** Moon, S., Perron, J. T., Martel, S. J., Goodfellow, B. W., Mas Ivars, D., Simeonov, A., Munier, R., Naslund, J.-O., Hall, A., Stroeven, A. P., Ebert, K., and Heyman, J.: Landscape features influence bedrock fracture openness in the deep subsurface, *Geological Society of American Annual Meeting*, Phoenix, AZ, USA, 10.1130/abs/2019AM-336309,
- 1429**
- 1430**
- 1431** Moser, F.: Spatial and temporal variance in rock dome exfoliation and weathering near Twain Harte, California, USA, *Geography and Earth Sciences*, The University of North Carolina Charlotte, ProQuest, 2017.
- 1432**
- 1433** Mushkin, A., Sagy, A., Trabelci, E., Amit, R., and Porat, N.: Measure the time and scale-dependency of subaerial rock weathering rates over geologic time scales with ground-based lidar, *Geology*, 42, 1063-1066, 2014.
- 1434**
- 1435** Nara, Y. and Kaneko, K.: Sub-critical crack growth in anisotropic rock, *International Journal of Rock Mechanics and Mining Sciences*, 43, 437-453, <https://doi.org/10.1016/j.ijrmms.2005.07.008>, 2006.
- 1436**
- 1437** Nara, Y., Kashiwaya, K., Nishida, Y., and Ii, T.: Influence of surrounding environment on subcritical crack growth in marble, *Tectonophysics*, 706-707, 116-128, 2017.
- 1438**
- 1439** Nara, Y., Morimoto, K., Hiroyoshi, N., Yoneda, T., Kaneko, K., and Benson, P. M.: Influence of relative humidity on fracture toughness of rock: Implications for subcritical crack growth, *International Journal of Solids and Structures*, 49, 2471-2481, <https://doi.org/10.1016/j.ijsolstr.2012.05.009>, 2012.
- 1440**
- 1441**
- 1442** Narr, W. and Lerche, I.: A method for estimating subsurface fracture density in core, *AAPG Bulletin*, 68, 637-648, 10.1306/ad461354-16f7-11d7-8645000102c1865d, 1984.
- 1443**
- 1444** Neely, A. B., DiBiase, R. A., Corbett, L. B., Bierman, P. R., and Caffee, M. W.: Bedrock fracture density controls on hillslope erodibility in steep, rocky landscapes with patchy soil cover, southern California, USA, *Earth and Planetary Science Letters*, 522, 186-197, <https://doi.org/10.1016/j.epsl.2019.06.011>, 2019.
- 1445**
- 1446**
- 1447** Ollier, C. D.: *Weathering*, 2nd, Longman, London, England, 1984.

- 1448** Olsen, T., Borella, J., and Stahl, T.: Clast transport history influences Schmidt hammer rebound values, *Earth Surface Processes and Landforms*, 45, 1392-1400, <https://doi.org/10.1002/esp.4809>, 2020.
- 1449**
- 1450** Olson, J. E.: Predicting fracture swarms - the influence of subcritical crack growth and the crack-tip process zone on joint spacing in rock, *Geological Society of London Special Publications*, 231, 73-87, 2004.
- 1451**
- 1452** Ortega, O. and Marrett, R.: Prediction of macrofracture properties using microfracture information, Mesaverde Group sandstones, San Juan basin, New Mexico, *Journal of Structural Geology*, 22, 571-588, [https://doi.org/10.1016/S0191-8141\(99\)00186-8](https://doi.org/10.1016/S0191-8141(99)00186-8), 2000.
- 1453**
- 1454** Ortega, O. J., Marrett, R. A., and Laubach, S. E.: A scale-independent approach to fracture intensity and average spacing measurement, *AAPG Bulletin*, 90, 193-208, 10.1306/08250505059, 2006.
- 1455**
- 1456** Paris, P. and Erdogan, F.: A critical analysis of crack propagation laws, *Journal of Basic Engineering*, 85, 528-533, 10.1115/1.3656900, 1963.
- 1457**
- 1458** Phillips, J. D.: An evaluation of the factors determining the effectiveness of water quality buffer zones, *Journal of Hydrology*, 107, 133-145, [https://doi.org/10.1016/0022-1694\(89\)90054-1](https://doi.org/10.1016/0022-1694(89)90054-1), 1989.
- 1459**
- 1460** Ponti, S., Pezza, M., and Guglielmin, M.: The development of Antarctic tafoni: Relations between differential weathering rates and spatial distribution of thermal events, salts concentration, and mineralogy, *Geomorphology*, 373, 2021.
- 1461**
- 1462** Ramcharan, A., Hengl, T., Nauman, T., Brungard, C., Waltman, S., Wills, S., and Thompson, J.: Soil property and class maps of the conterminous United States at 100-meter spatial resolution, *Soil Science Society of America Journal*, 82, 186-201, <https://doi.org/10.2136/sssaj2017.04.0122>, 2018.
- 1463**
- 1464**
- 1465** Ramulu, M., Chakraborty, A. K., and Sitharam, T. G.: Damage assessment of basaltic rock mass due to repeated blasting in a railway tunnelling project – A case study, *Tunnelling and Underground Space Technology*, 24, 208-221, <https://doi.org/10.1016/j.tust.2008.08.002>, 2009.
- 1466**
- 1467**
- 1468** Rasmussen, M., Eppes, M. C., and Berberich, S.: Untangling the impacts of climate, lithology, and time on rock cracking rates and morphology in arid and semi-arid Eastern California, *AGU Fall Meeting*, New Orleans, LA, 2021.
- 1469**
- 1470** Ravaji, B., Ali-Lagoa, V., Delbo, M., and Wilkerson, J. W.: Unraveling the mechanics of thermal stress weathering rate-effects, size-effects, and scaling laws., *Journal of Geophysical Research*, 121, 3304-3328, 10.1029/2019JE006019, 2019.
- 1471**
- 1472** Riebe, C. S., Callahan, R. P., Granke, S. B.-M., Carr, B. J., Hayes, J. L., Schell, M. S., and Sklar, L. S.: Anisovolumetric weathering in granitic saprolite controlled by climate and erosion rate, *Geology*, 1-5, 10.1130/G48191.1, 2021.
- 1473**
- 1474** Rossen, W. R., Gu, Y., and Lake, L. W.: Connectivity and permeability in fracture networks obeying power-law statistics, *SPE Permian Basin Oil and Gas Recovery Conference*, 10.2118/59720-ms, 2000.
- 1475**
- 1476** Røyne, A., Jamtveit, B., Mathiesen, J., and Malthe-Sørenssen, A.: Controls on rock weathering rates by reaction-induced hierarchical fracturing, *Earth and Planetary Science Letters*, 275, 364-369, <https://doi.org/10.1016/j.epsl.2008.08.035>, 2008.
- 1477**
- 1478** Rysak, B., Gale, J. F., Laubach, S. E., & Ferrill, D. A.: Mechanisms for the generation of complex fracture networks: Observations from slant core, analog models, and outcrop, *Frontiers in Earth Science*, 10, 848012, 2022.
- 1479**
- 1480** Sanderson, D. J.: Field-based structural studies as analogues to sub-surface reservoirs, *Geological Society, London, Special Publications*, 436, 207-217, doi:10.1144/SP436.5, 2016.
- 1481**
- 1482** Sanderson, D. J. and Nixon, C. W.: Topology, connectivity and percolation in fracture networks, *Journal of Structural Geology*, 115, 167-177, <https://doi.org/10.1016/j.jsg.2018.07.011>, 2018.
- 1483**
- 1484** Scarciglia, F., Saporito, N., La Russa, M. F., Le Pera, E., Macchione, M., Puntillo, D., Crisci, G. M., and Pezzino, A.: Role of lichens in weathering of granodiorite in the Sila uplands (Calabria, Southern Italy), *Sedimentary Geology*, 280, 119-134, 2012.
- 1485**
- 1486** Schoeneberger, P. J., Wysocki, D. A., and Benham, E. C.: *Field Book for Describing and Sampling Soils: Version 3.0*, Natural Resources Conservation Service, National Soil Survey Center, Lincoln, Nebraska 2012.
- 1487**
- 1488** Schultz, R. A.: *Geologic Fracture Mechanics*, Cambridge University Press, Cambridge, England, DOI: 10.1017/9781316996737, 2019.
- 1489**
- 1490** Shakiba, M., Lake, L.W., Gale, J.F.W., Laubach, S.E., Pyrcz, M.J.: Multiscale spatial analysis of fracture nodes in two dimensions, *Marine & Petroleum Geology*, 149, 106093, doi.org/10.1016/j.marpetgeo.2022.106093, 2023.
- 1491**
- 1492** Sharifigaliuk, H., Mahmood, S. M., Ahmad, M., and Rezaee, R.: Use of outcrop as substitute for subsurface shale: Current understanding of similarities, discrepancies, and associated challenges, *Energy & Fuels*, 35, 9151-9164, 10.1021/acs.energyfuels.1c00598, 2021.
- 1493**
- 1494**

- 1495** Shi, J.: Study of thermal stresses in rocks due to diurnal solar exposure, Civil Engineering, University of Washington, 58 pp., 2011.
- 1496** Shobe, C. M., Hancock, G. S., Eppes, M. C., and Small, E. E.: Field evidence for the influence of weathering on rock erodibility and channel form in bedrock rivers, *Earth Surface Processes and Landforms*, 42, 1997-2012, 2017.
- 1497**
- 1498** Sklar, L. S., Riebe, C. S., Marshall, J. A., Genetti, J., Leclere, S., Lukens, C. L., and Merces, V.: The problem of predicting the size distribution of sediment supplied by hillslopes to rivers, *Geomorphology*, 277, 31-49, 2017.
- 1499**
- 1500** Snowdon, A. P., Normani, S. D., and Sykes, J. F.: Analysis of crystalline rock permeability versus depth in a Canadian Precambrian rock setting, *Journal of Geophysical Research: Solid Earth*, 126, e2020JB020998, <https://doi.org/10.1029/2020JB020998>, 2021.
- 1501**
- 1502** Sousa, L. M. O.: Evaluation of joints in granitic outcrops for dimension stone exploitation, *Quarterly Journal of Engineering Geology and Hydrogeology*, 43, 85-94, 10.1144/1470-9236/08-076, 2010.
- 1503**
- 1504** St. Clair, J., Moon, S., Holbrook, W. S., Perron, J. T., Riebe, C. S., Martel, S. J., Carr, B., Harman, C., Singha, K., and Richter, D. D.: Geophysical imaging reveals topographic stress control of bedrock weathering, *Geomorphology*, 350, 534-538, 2015.
- 1505**
- 1506** Staff, Soil Survey: Soil Taxonomy: A basic system of soil classification for making and interpreting soil surveys, 1999.
- 1507** R.D. Terzaghi: Sources of error in joint surveys, *Geotechnique*, 15, 287-304, 1965.
- 1508** Terry, R. D. and Chilingar, G. V.: Summary of "Concerning some additional aids in studying sedimentary formations," by M. S. Shvetsov, *Journal of Sedimentary Research*, 25, 229-234, 10.1306/74d70466-2b21-11d7-8648000102c1865d, 1955.
- 1509**
- 1510** Turner, F. J., Griggs, D. T., and Heard, H. C.: Experimental deformation of calcite crystals, *GSA Bulletin*, 65, 883-934, 10.1130/0016-7606(1954)65[883:Edocc]2.0.Co;2, 1954.
- 1511**
- 1512** Ukar, E., Laubach, S. E., and Hooker, J. N.: Outcrops as guides to subsurface natural fractures: Example from the Nikanassin Formation tight-gas sandstone, Grande Cache, Alberta foothills, Canada, *Marine and Petroleum Geology*, 103, 255-275, <https://doi.org/10.1016/j.marpetgeo.2019.01.039>, 2019.
- 1513**
- 1514**
- 1515** Ulusay, R. and Hudson, J. A.: The Complete ISRM Suggested Methods for Rock Characterization, Testing and Monitoring: 1974-2006, Commission on Testing Methods, International Society of Rock Mechanics., Ankara, Turkey2007.
- 1516**
- 1517** Ulusay, R (ed.), 2015. The ISRM suggested methods for rock characterization, testing and monitoring: 2007–2014. Springer, Cham, Switzerland. DOI:10.1007/978-3-319-007713-0."Vazquez, P., Shushakova, V., and Gomez-Heras, M.: Influence of mineralogy on granite decay induced by temperature increase: Experimental observations and stress simulation, *Engineering Geology*, 189, 58-67, 2015.
- 1518**
- 1519**
- 1520**
- 1521** Viswanathan, H.S., et al: From fluid flow to coupled processes in fractured rock: recent advances and new frontiers, *Reviews of Geophysics*, 60(1), e2021RG000744, 2022.
- 1522**
- 1523** Wang, H. F., Bonner, B. P., Carlson, S. R., Kowallis, B. J., and Heard, H. C.: Thermal stress cracking in granite, *Journal of Geophysical Research: Solid Earth*, 94, 1745-1758, <https://doi.org/10.1029/JB094iB02p01745>, 1989.
- 1524**
- 1525** Wang, Q., Narr, W., Laubach, S.E.: Quantitative characterization of fracture spatial arrangement and intensity in a reservoir anticline using horizontal wellbore image logs and an outcrop analog, *Marine & Petroleum Geology*, 152, 106238, <https://doi.org/10.1016/j.marpetgeo.2023.106238>, 2023.
- 1526**
- 1527**
- 1528** Watkins, H., Bond, C. E., Healy, D., and Butler, R. W. H.: Appraisal of fracture sampling methods and a new workflow to characterise heterogeneous fracture networks at outcrop, *Journal of Structural Geology*, 72, 67-82, <https://doi.org/10.1016/j.jsg.2015.02.001>, 2015.
- 1529**
- 1530**
- 1531** Weiserbs, B. I.: The morphology and history of exfoliation on rock domes in the Southeastern United States, *Geography and Earth Sciences*, The University of North Carolina Charlotte, ProQuest, 2017.
- 1532**
- 1533** Weiss, M.: Techniques for estimating fracture size: A comparison of methods, *International Journal of Rock Mechanics and Mining Sciences*, 45, 460-466, <https://doi.org/10.1016/j.ijrmms.2007.07.010>, 2008.
- 1534**
- 1535** Wenk, H.-R.: Some roots of experimental rock deformation, *Bulletin de Mineralogie*, 102, 195-202, <https://doi.org/10.3406/bulmi.1979.7277>, 1979.
- 1536**
- 1537** West, N., Kirby, E., Bierman, P. R., and Clarke, B. A.: Aspect-dependent variations in regolith creep revealed by meteoric <sup>10</sup>Be, *Geology*, 42, 507-510, 10.1130/g35357.1, 2014.
- 1538**
- 1539** Wohl, E. E.: The effect of bedrock jointing on the formation of straths in the Cache la Poudre River drainage, Colorado Front Range, *Journal of Geophysical Research: Earth Surface*, 113, <https://doi.org/10.1029/2007JF000817>, 2008.
- 1540**

- 1541** Wolman, M. G.: A method of sampling coarse river-bed material, *Eos, Transactions American Geophysical Union*, 35, 951-956,  
**1542** <https://doi.org/10.1029/TR035i006p00951>, 1954.
- 1543** Wu, H. and Pollard, D. D.: An experimental study of the relationship between joint spacing and layer thickness, *Journal of*  
**1544** *Structural Geology*, 17, 887-905, [https://doi.org/10.1016/0191-8141\(94\)00099-L](https://doi.org/10.1016/0191-8141(94)00099-L), 1995.
- 1545** Zeeb, C., Gomez-Rivas, E., Bons, P. D., and Blum, P.: Evaluation of sampling methods for fracture network characterization using  
**1546** outcrops, *AAPG Bulletin*, 97, 1545-1566, 10.1306/02131312042, 2013.
- 1547** Zeng, Fan, Biao Shu, and Qiwu Shen. "A combination of Light Detection and Ranging with Digital Panoramic Borehole Camera  
**1548** System in fracture mapping to characterize discrete fracture networks." *Bulletin of Engineering Geology and the Environment* 82,  
**1549** no. 7, 249, <https://doi.org/10.1007/s10064-023-03274-5> , 2023:
- 1550** Zhang, C., Hu, X., Wu, Z., and Li, Q.: Influence of grain size on granite strength and toughness with reliability specified by normal  
**1551** distribution, *Theoretical and Applied Fracture Mechanics*, 96, 534-544, <https://doi.org/10.1016/j.tafmec.2018.07.001>, 2018.
- 1552** Zhang, L.: Determination and applications of rock quality designation (RQD), *Journal of Rock Mechanics and Geotechnical*  
**1553** *Engineering*, 8, 389-397, <https://doi.org/10.1016/j.jrmge.2015.11.008>, 2016.
- 1554** Zhou, W., Shi, G., Wang, J., Liu, J., Xu, N., and Liu, P.: The influence of bedding planes on tensile fracture propagation in shale  
**1555** and tight sandstone, *Rock Mechanics and Rock Engineering*, 55, 1111-1124, 10.1007/s00603-021-02742-2, 2022.
- 1556**

FIGURE 1

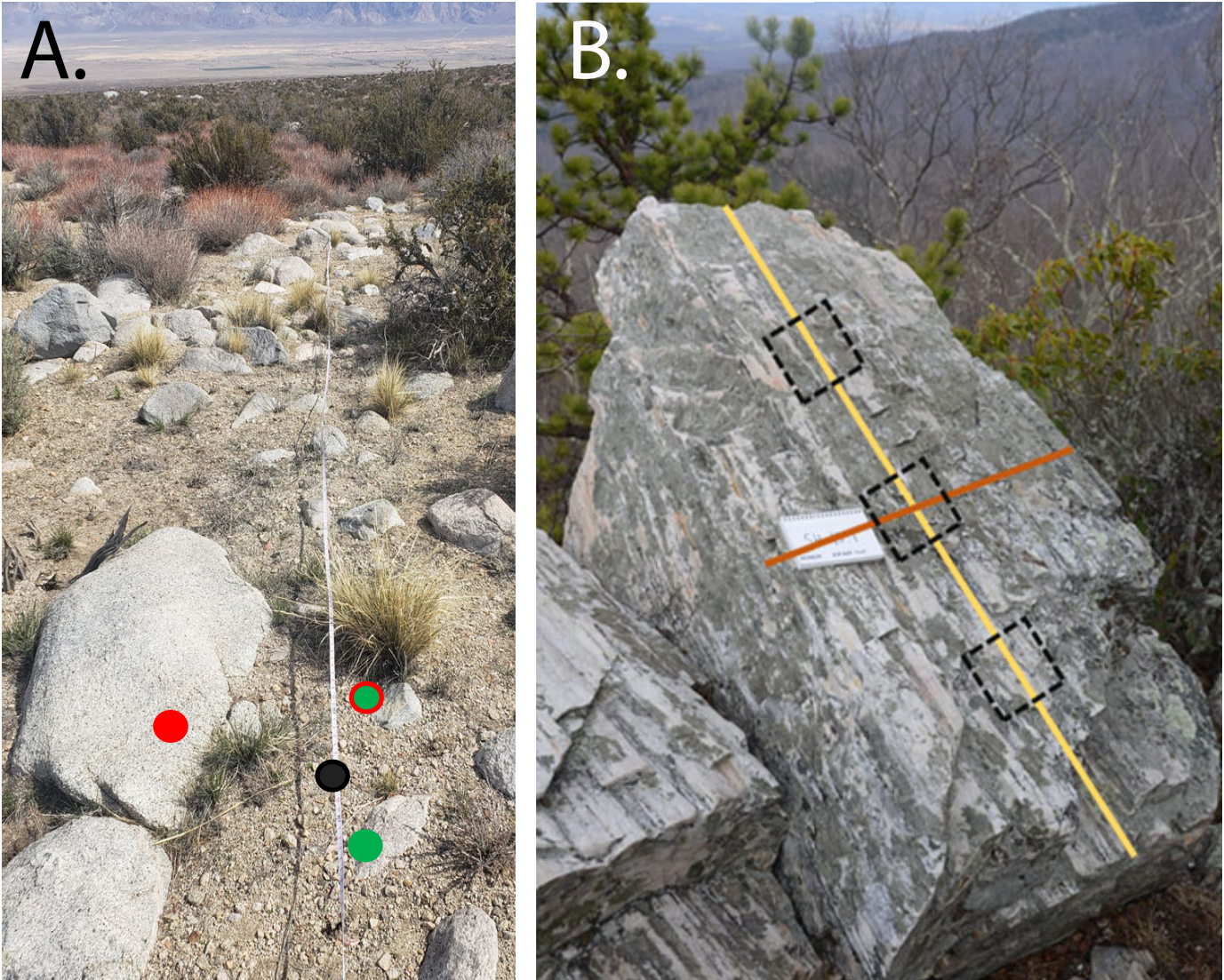


Fig. 1. Images illustrating the selection of observation areas for clasts and outcrops. A. Photograph of a transect established for clast selection. Black dot: predefined transect interval location on the tape. Red dot: clast that does not fit the predefined clast selection criteria (e.g., it is too big). Green dot with red circle: clast that fits criteria but is further away from the interval point than the clast with the green dot. Green dot: closest clast to the transect interval that meets the selection criteria. B. Annotated photograph showing an idealized placement of 'windows' (dashed black squares) on a bedrock outcrop. Outcrop dimensions are measured and the windows are placed using predetermined selection criteria. In this example, the windows are equally spaced along the centerline of the long-dimension of the upward-facing side of the outcrop.

Fig. 2. A. Example of the measurement of a surface exposure length (L; yellow line) of a fracture meeting the criteria in Table 1. The 'h' refers to the location where sheet height would be measured for this surface parallel fracture. B. Example of fractures that may appear to be a single fracture (left), but upon close examination are in fact multiple fractures intersecting and/or separated by rock (right inset). Arrow points to the location of the inset image on the main image. Compass in the foreground for scale.

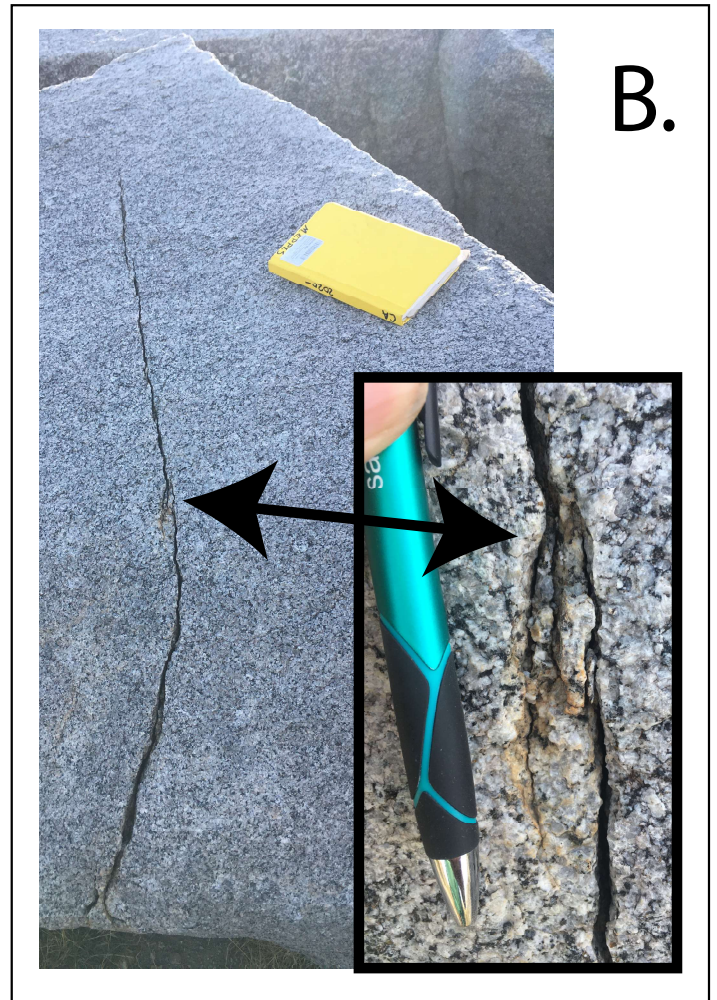
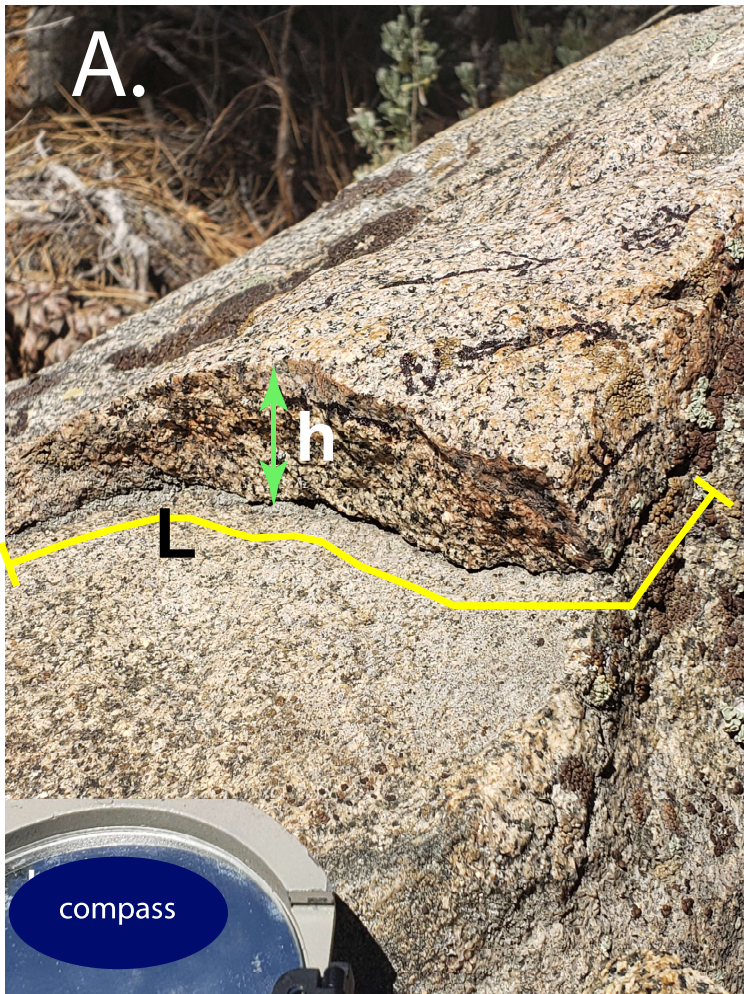


FIGURE 3

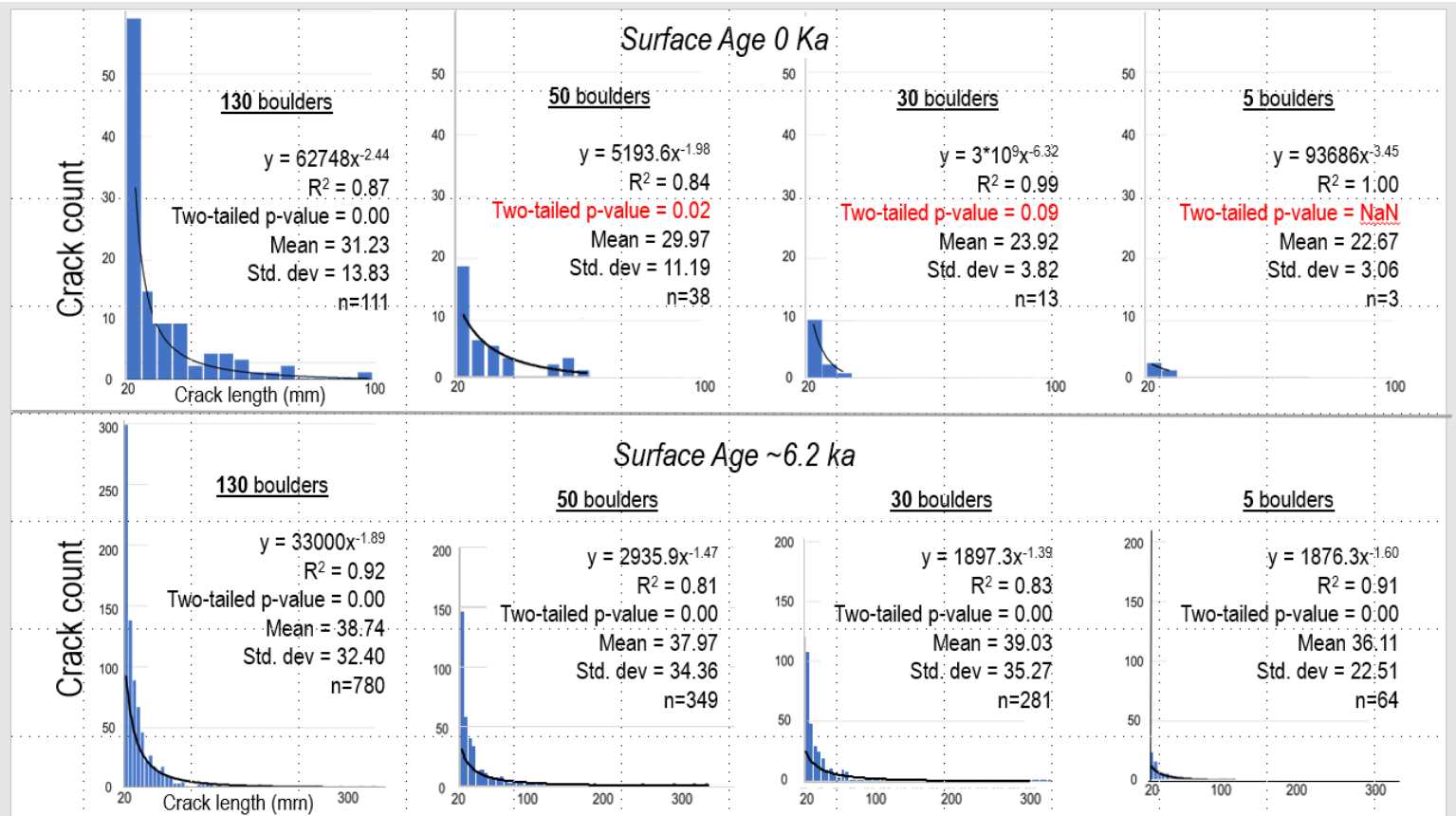


Fig. 3

Fig. 3. Example histograms and statistics of fracture length data measured on the exposed surfaces of clasts 15-50 cm max diameter. Upper row are data for clasts found on a modern ephemeral stream boulder bar. Clasts overall have very low fracture number density. Lower row are data for clasts on an ~6 ka surface where fracture number density is much higher. Note that it takes about 100 clasts to arrive at a statistically significant power law distribution for the Modern Wash clasts, but only 5 rocks for the rocks with higher fracture densities. Producing histograms interactively as data is collected can help establish how many observation areas are necessary for a given site.

FIGURE 4

Name(s) & Date:		Criteria for Clast/Outcrop selection:										Relevant Cl, O, R, P, T observations:									
Site Name:												Vegetation-type & percent of each:									
GPS Coordinates:												open ground cover (%):									
GPS Projection:		Portion observed (eg. All exposed, north face only, etc.):										Surface Slope:									
Orientation conventions:												Other:									
Declination:																					

ID & Rock Type	Avg. Grain Size (mm)	sphericity/roundness	Mineralogy	Length (cm)	Width (cm)	Height (cm)	Exposure	Cracks cm	GD & Pit	Lichen	Varnish	Fabric Type	Fabric Strike (°)	Fabric Dip (°)	Crack ID	Crack Parallel to	Mid Crack Width (mm)	Crack Max Width (mm)	Crack Length ( mm )	Crack Strike (°)	Crack Dip (°)	Sheet Ht. (mm)	Weathering Index	Notes	
s- r-							0123	012345	gp	012345	012345	FSBVO				SFL							1 2 3 4 5		
s- r-							0123	012345	gp	012345	012345	FSBVO				SFL								1 2 3 4 5	
s- r-							0123	012345	gp	012345	012345	FSBVO				SFL								1 2 3 4 5	
s- r-							0123	012345	gp	012345	012345	FSBVO				SFL								1 2 3 4 5	
s- r-							0123	012345	gp	012345	012345	FSBVO				SFL								1 2 3 4 5	
s- r-							0123	012345	gp	012345	012345	FSBVO				SFL								1 2 3 4 5	
s- r-							0123	012345	gp	012345	012345	FSBVO				SFL								1 2 3 4 5	
s- r-							0123	012345	gp	012345	012345	FSBVO				SFL								1 2 3 4 5	
s- r-							0123	012345	gp	012345	012345	FSBVO				SFL								1 2 3 4 5	
s- r-							0123	012345	gp	012345	012345	FSBVO				SFL								1 2 3 4 5	
s- r-							0123	012345	gp	012345	012345	FSBVO				SFL								1 2 3 4 5	
s- r-							0123	012345	gp	012345	012345	FSBVO				SFL								1 2 3 4 5	
s- r-							0123	012345	gp	012345	012345	FSBVO				SFL								1 2 3 4 5	
s- r-							0123	012345	gp	012345	012345	FSBVO				SFL								1 2 3 4 5	
s- r-							0123	012345	gp	012345	012345	FSBVO				SFL								1 2 3 4 5	
s- r-							0123	012345	gp	012345	012345	FSBVO				SFL								1 2 3 4 5	
s- r-							0123	012345	gp	012345	012345	FSBVO				SFL								1 2 3 4 5	
s- r-							0123	012345	gp	012345	012345	FSBVO				SFL								1 2 3 4 5	
s- r-							0123	012345	gp	012345	012345	FSBVO				SFL								1 2 3 4 5	
s- r-							0123	012345	gp	012345	012345	FSBVO				SFL								1 2 3 4 5	
s- r-							0123	012345	gp	012345	012345	FSBVO				SFL								1 2 3 4 5	
s- r-							0123	012345	gp	012345	012345	FSBVO				SFL								1 2 3 4 5	
s- r-							0123	012345	gp	012345	012345	FSBVO				SFL								1 2 3 4 5	
s- r-							0123	012345	gp	012345	012345	FSBVO				SFL								1 2 3 4 5	
s- r-							0123	012345	gp	012345	012345	FSBVO				SFL								1 2 3 4 5	
s- r-							0123	012345	gp	012345	012345	FSBVO				SFL								1 2 3 4 5	
s- r-							0123	012345	gp	012345	012345	FSBVO				SFL								1 2 3 4 5	
s- r-							0123	012345	gp	012345	012345	FSBVO				SFL								1 2 3 4 5	

**Cracks <2 cm:** Evidence of microcracks <2 cm long, 0 = 0; 1 = <1/dm<sup>2</sup>; 2 = 1-5/dm<sup>2</sup>; 3 = 5-10/dm<sup>2</sup>; 4 = 210/dm<sup>2</sup>

**GD & Pit:** G = positive evidence of granular disintegration (loose grains) P = pitting evident

**Crack Length:** defined as total exposed length of the crack; equivalent to a surface exposure length NOT a 'caliper' length.

**Fabric type:** f=foliation; s=fossils; b=bedding; v = vein or dyke o=other

**Lichen & varnish:** 0 = 0%, 1 => 0 and <10; 2 => 10 and <30; 3 => 30 and <60; 4 = >60 and <90; 5 => 90

**Avg. Grain Size** = representative size of grains throughout the boulder

**Parallel:** S = surface, F = fabric, L = long axis of clast or outcrop

**Sheet Ht** = the height of the spall or exfoliation resulting from a surface-parallel crack; n/a for other cracks

**Crack Parallel to:** S: Surface, F: Fabric (joints, bedding); L: long axis

**weathering Index:**

0 = no crack (step)

1: fresh with evidence of recent rupture (flakes/pieces)

2: sharp, no rounded edges anywhere

3: mostly sharp with occasional rounded edges

4: mostly rounded edges with occasional sharp

5: all rounded edges

**NOTE:** 0, or 1 must have clear evidence of a recent break: i.e. small pieces left

**Exposure**  
use angle of the boulder at the ground

Fig. 4. Reduced size image of an 8.5” x 11” ‘fracture sheet’ to be employed in the field to increase efficiency and to reduce ‘missing’ data. Sheet templates for both clasts and outcrops that can be modified are provided in Data Supplement as well as a data-entry template.



FIGURE 5

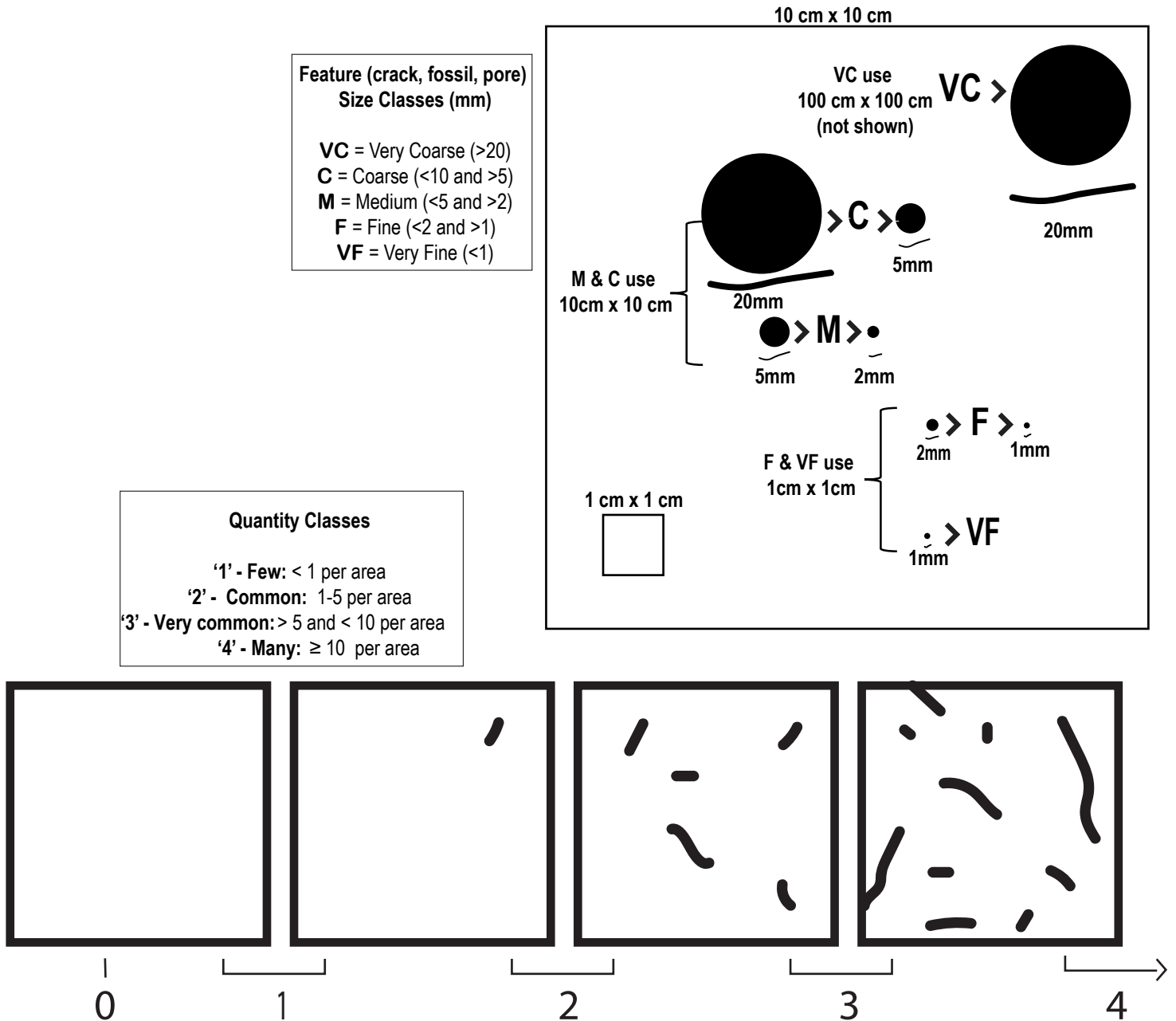


Fig. 5. Visual aid for estimating the abundance of “countable” rock features – including fractures. An index of 0-4 is assigned depending on the abundance of features within an average of any given observation area (ex: 10 x 10 cm) on the clast or window being examined. The area of observation is defined by the size of the features being measured. A 10 cm x 10 cm square is used for estimating the abundance of ‘fractures < 2 cm’ defined as fractures with lengths of >0.5 cm but < 2 cm (see section 5.2 for details of how to use the index). For features ≤0.5 cm, a 1 cm x 1 cm area would be employed and for features ≥2 cm, a 1 x 1 m area. Ensure the image is printed to scale prior to use in the field.

FIGURE 6

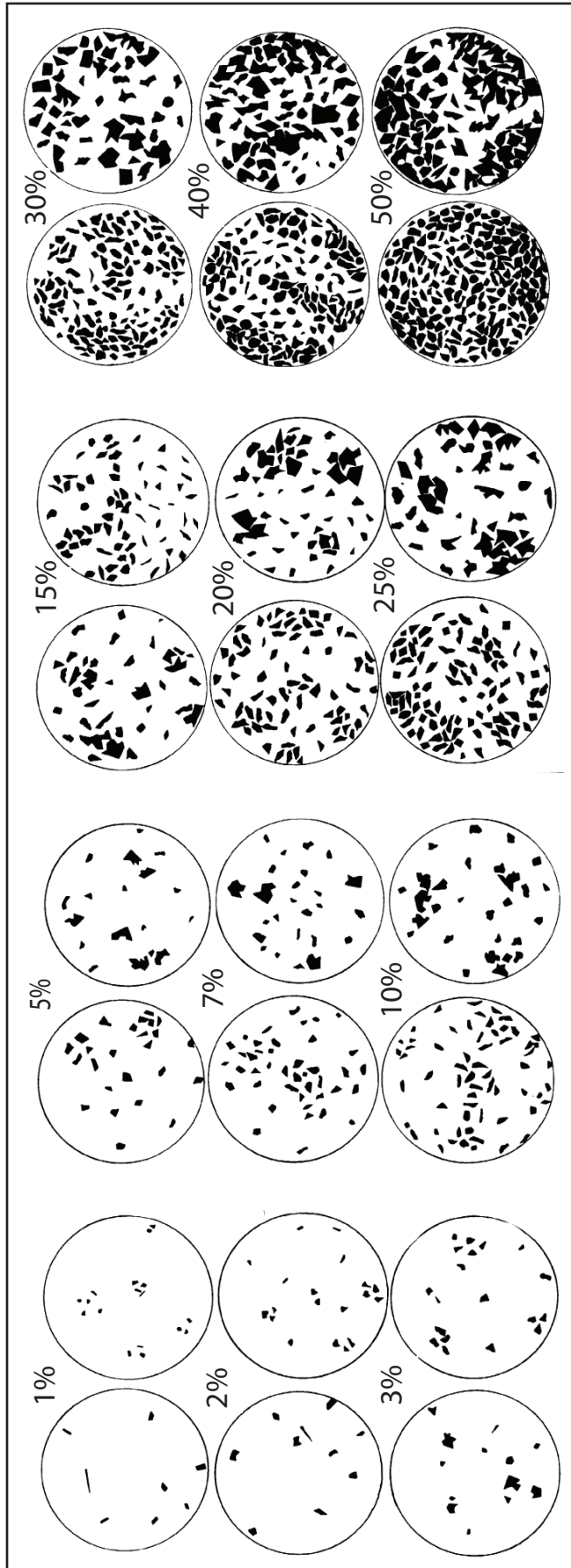
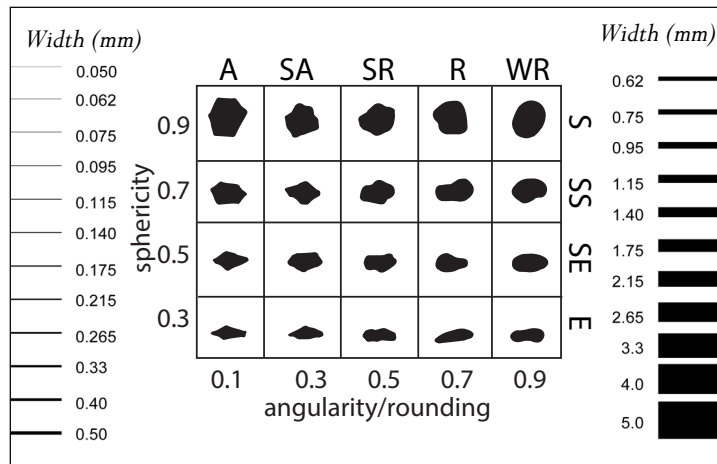


Fig. 6. A visual percent estimator (modified from Terry and Chilingar, 1955). Estimator should be employed in every estimate of percentages. See section 5.2 for using the estimator to assign a percent coverage index to features that are not countable or vary in size (e.g., lichen coverage, fine mafic minerals, etc.).

FIGURE 7



note to copy-editor: this figure should be published to scale when the document is viewed at 100%

Fig. 7. Inset: Roundness and sphericity chart – modified from Krumbein and Sloss (1951) to add the roundness and sphericity lettering. Roundness: A = angular; SA = subangular; SR = subrounded; R = rounded; WR = well-rounded. Sphericity: S = spherical; SS = subspherical; SE = sub-elongate; E = elongate. Edges: fracture comparator whereby the width most closely matching the fracture aperture is noted. Note: a to-scale pdf is available in the Data Supplement, however, owing to printing and publication scaling, it is highly recommended to calibrate the comparator prior to using it in the field.

FIGURE 8

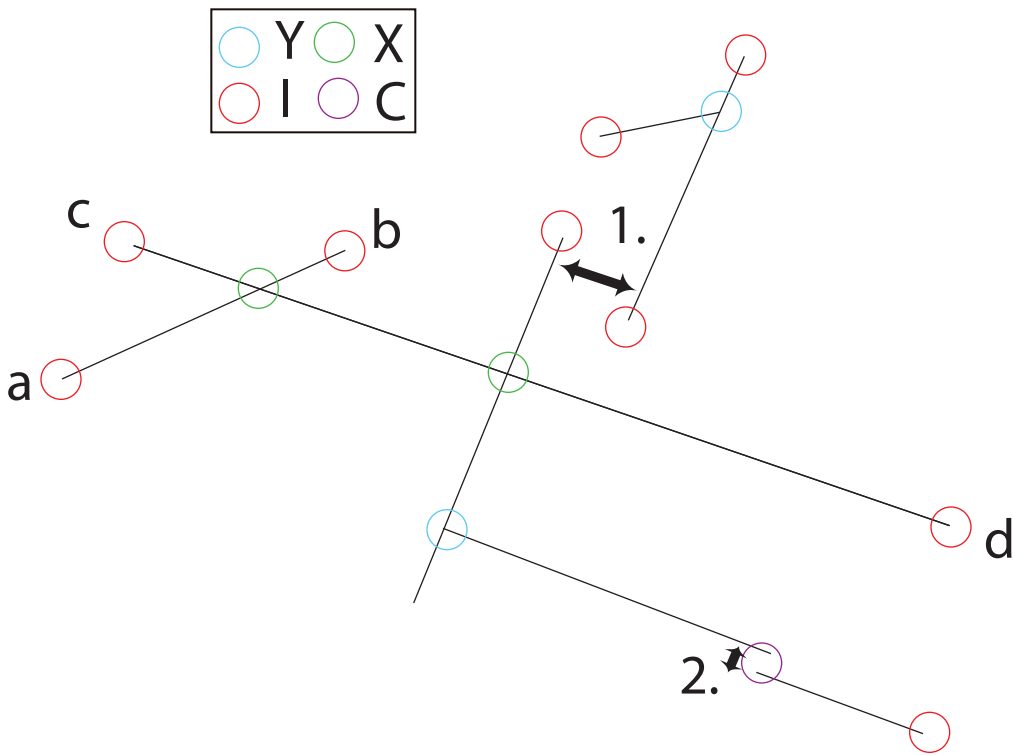


Fig. 8 Depiction of types of fracture intersection nodes. I-nodes comprise fracture terminations with no connections. Y-nodes are abutting fractures that do not cross. X-nodes are fractures that cross. C-nodes are 'contingent nodes' defined by the user. In this example the rule is related to the distance between I-nodes. For #1, the distance is wider than the criteria, so the terminations are designated as I-nodes. For #2, the distance is within the limits, and the 'connection' is designated as a C-node.

FIGURE 9

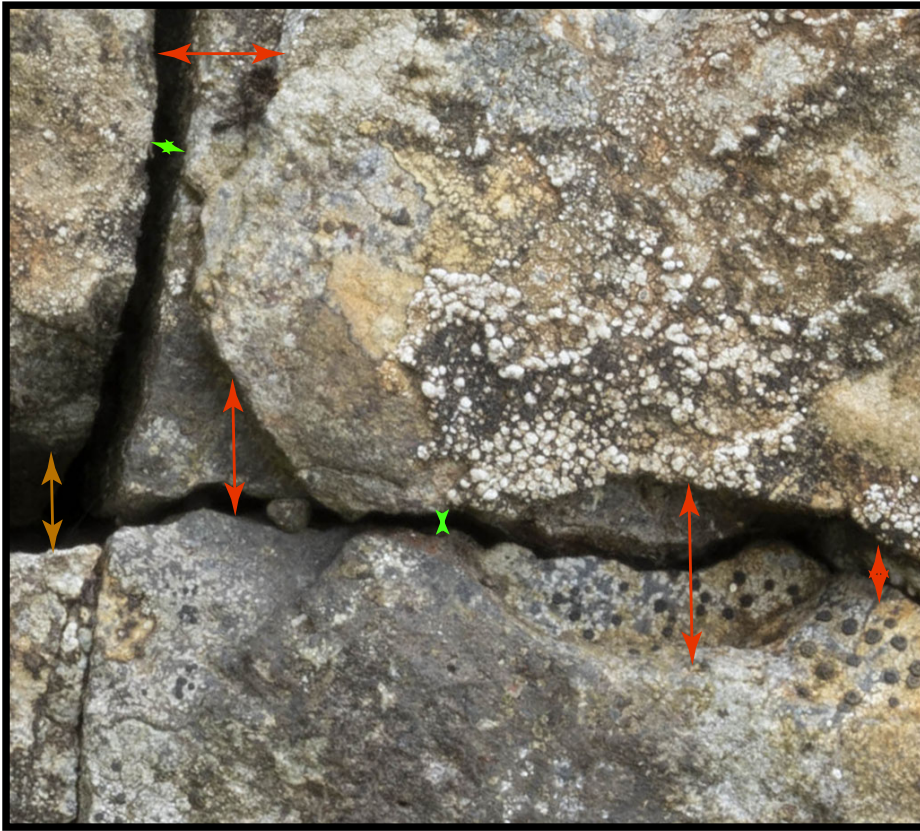


Fig. 9. Examples of aperture transects that are appropriate for measurement of fracture aperture widths (green) and transects where there is evidence that the fracture walls have been eroded or chipped and therefore should not be employed for a width measurement (red). In cases where it is not clear if erosion or chipping has occurred (orange), a note can be made for the fracture width to possibly eliminate outliers during data analysis.

FIGURE 10

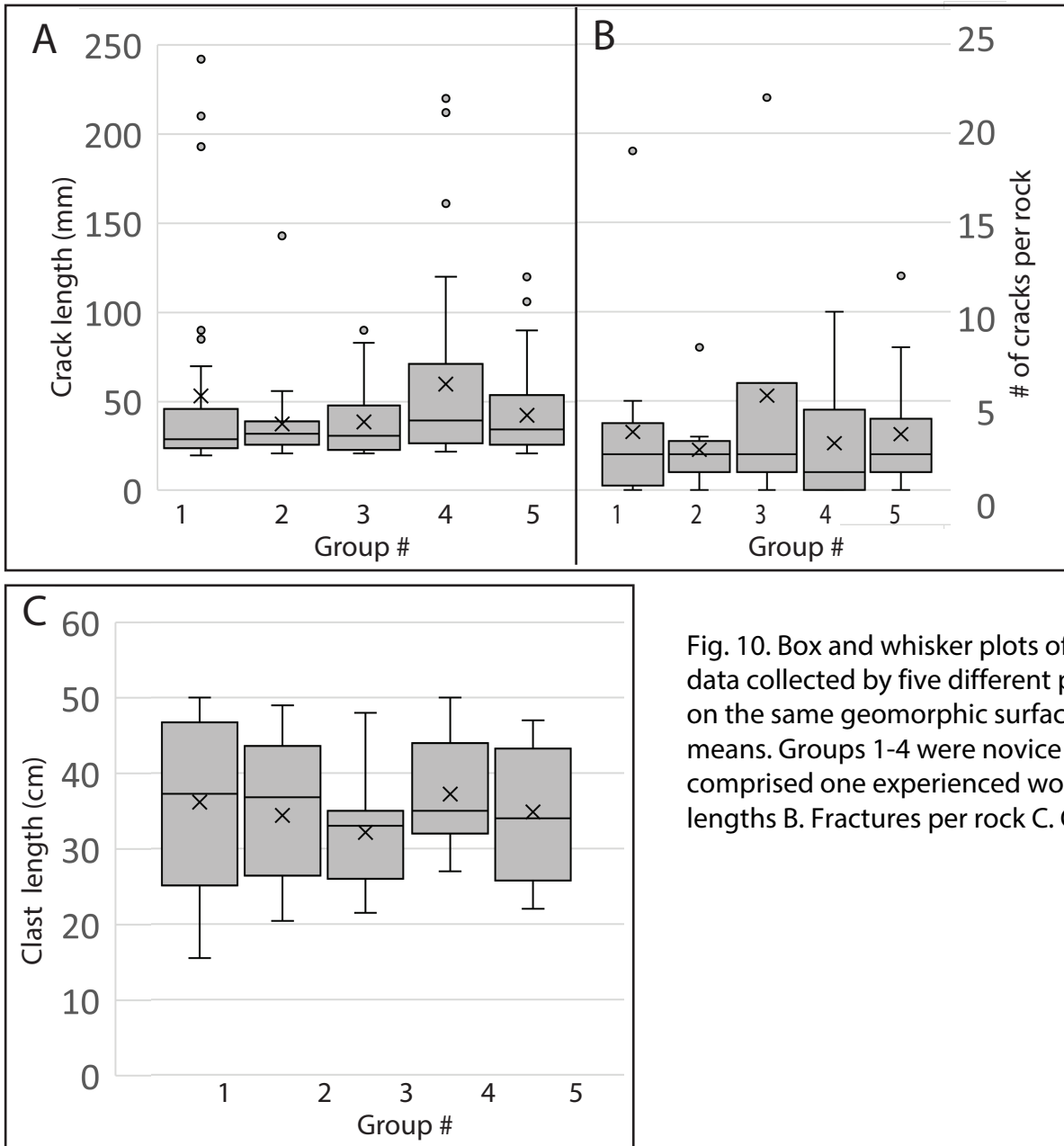


Fig. 10. Box and whisker plots of case example data collected by five different pairs of workers on the same geomorphic surface. "x"s mark the means. Groups 1-4 were novice workers. Group 5 comprised one experienced worker. A. Fracture lengths B. Fractures per rock C. Clast length